Revisiting the trafficking of insulin and its receptor in rat liver: *in vivo* and cell-free studies

Khadija Tahiri, Françoise Fouque, Marie-Catherine Postel-Vinay and Bernard Desbuquois

Abstract

Endosomes are the main locus where, upon endocytosis in liver cells, insulin and the activated insulin receptor accumulate and insulin is degraded. In this study, ligand and receptor pathways in rat liver have been revisited using analytical subcellular fractionation. Density gradient analysis of microsomal and light mitochondrial fractions confirmed that, upon *in vivo* uptake into liver, [^{125}I]-insulin was rapidly translocated from plasma membranes to endosomes. Internalized [^{125}I]-labeled proinsulin and biotinylated insulin, which are less degraded than insulin in endosomes, were in part transferred to lysosomes. Following injection of native insulin, receptor and ligand were also both translocated from the plasma membrane to endosomes, with a maximum at 15-30 min. Receptor translocation was reversed by 2-3 hours and neither endocytosis nor recycling were affected by *in vivo* cycloheximide treatment. Fractionation of endosomes of insulin-treated rats on density gradients showed that the insulin receptor was recovered at low density, whereas insulin progressively migrated from low to high densities towards the position of acid phosphatase. On SDS polyacrylamide gels, insulin receptor α and β subunits were identified in plasma membrane, endosomal and lysosomal fractions by affinity crosslinking and Western immunoblotting, respectively. Following insulin treatment, insulin receptor expression rapidly decreased in plasma membranes while increasing in endosomes. In a cell-free system, [^{125}I]-insulin was in part transferred from endosomes to lysosomes, as was, with organelle content mixing, [^{125}I]-biotinylated insulin. In summary: 1) the low lysosomal association of [^{125}I]-insulin *in vivo* is linked to its endosomal degradation; 2) upon ligand-induced endocytosis, the insulin receptor progressively segregates from insulin and is recycled; 3) neither endocytosis no recycling of the receptor requires protein synthesis.

Abbreviations:

Akt, Akt serine/threonine kinase, APS, adaptor protein with PH and SH2 domains; CEACAM, carcino-embryonic antigen-related cell adhesion molecule; DSS, disuccinimidyl suberate; galBSA, galactosylated bovine serum-albumin; Grb, growth factor receptor bound protein; IRS, insulin receptor substrate; PC-1/ENPP1, plasma cell membrane glycoprotein 1/ectonucleotide pyrophosphatase phosphodiesterase 1; PI3K, phosphoinositide-3-kinase; Shc, Src homologous and collagen protein; SOCS, suppressor of cytokine signaling; SPDP, N-succinimidyl 3-(2-pyridyldithio) propionate; WGA, wheat germ agglutinin.

Introduction

Liver expresses specific, high affinity insulin receptors which mediate insulin action as well as degradation. Using as ligand [^{125}I]-insulin, liver insulin receptors were identified initially in plasma membrane (Freychet *et al*, 1971) and microsomal fractions (Cuatrecasas *et al*, 1971, 1972), and later in Golgi fractions (Bergeron *et al* 1973, Posner *et al,* 1978), nuclei and nuclear envelope (Goldfine & Smith 1976, Vigneri *et al*, 1978, Wong *et al* 1988), and isolated hepatocytes (Terris & Steiner, 1975, Olefsky *et al,* 1975). Shortly thereafter, morphological (Bergeron *et al*, 1977, 1979, Carpentier *et al*, 1979, Goldfine *et al,* s 1981) and biochemical (Desbuquois *et al*, 1979, 1982, Posner *et al*, 1980, Smith & Peters, 1982, Pease *et al*, 1985, 1987) studies showed that, upon *in vivo* receptor-mediated uptake into liver, [^{125}I]-insulin undergoes endocytosis along with the insulin receptor. This process, mainly clathrin-dependent, involves the translocation of the insulin-receptor complex from the plasma membrane to endosomes (reviewed by Bergeron *et al*, 1985). Liver insulin receptors were also shown to undergo ligand-induced translocation from the cell surface to nuclei (Podlecki *et al*, 1987, Wong *et al,* 1988, Gletsu *et al* 1999, Nelson *et al*, 2011, Kesten *et al* 2018). Endocytosis of the insulin-receptor complex is implicated in insulin degradation, signaling and action (reviewed by Knutson, 1991a, Morcavallo *et al,* 2014, Bergeron *et al*, 2016, Petersen *et al*, 2018, Chen *et al*, 2019, Hall *et al*, 2020, Iraburu *et al*, 2021).

Instead of lysosomes, in which many proteins taken up into liver are degraded, endosomes are the main site at which, upon dissociation of the internalized insulin-receptor complex, insulin is degraded (reviewed by Authier *et al,* 1994, and Berg *et al,* 1995). Studies on cell-free systems have shown that [^{125}I]-insulin degradation in liver endosomes occurs at low pH (4-5.5) and is functionally linked to ATP-dependent acidification by the vacuolar H(+)-ATPase proton pump (Pease *et al,* 1985, 1987, Smith *et al,* 1982, 1989, Doherty *et al*,

1990, Desbuquois *et al* 1990, 1992, Hamel *et al,* 1991, Bevan *et al,* 2000). Thus, degradation of [^{125}I]-insulin in isolated endosomes is inhibited by ionophores (nigericin, monensin), weak bases (chloroquine) and ATPase inhibitors (N-ethylmaleimide). Owing to its ability to inhibit degradation, *in vivo* chloroquine treatment increases the association of [^{125}I]-insulin with liver endosomes (Posner *et al,* 1982, Desbuquois *et al,* 1992) and extends the lifetime of the activated insulin receptor (Bevan *et al,* 1997). *In vitro* endosomal degradation of insulin is also inhibited by metal chelating agents (1,10-phenanthroline), thiol-blocking agents (p-chloro-mercuric benzoate) and the peptide antibiotic bacitracin (Peavy *et al,* 1985)

Degradation products of [^{125}I]-insulin in intact liver endosomes (Hamel *et al*, 1988, Clot *et al*, 1990, Seabright *et al*, 1992) and of native insulin in endosomal extracts (Authier *et al*, 2001) have been isolated and characterized, and sites at which insulin A and B chains of are cleaved have been identified. Insulin degrading enzyme (IDE), a neutral thiol metallo-endopeptidase, has been implicated in insulin degradation in endosomes (Duckworth, 1988, 1998, Najjar, 2018, Leissring, 2021) and proposed to initiate this process when insulin is still bound to its receptor. However, liver-specific ablation of IDE in mice did not affect insulin clearance (Villa-Perez *et al,* 2018), and based on crosslinking, immune-depletion and immune-blotting procedures, IDE has been localized in cytosol and peroxisomes but not in endosomes (Authier *et al*, 1994, 1995, 1996). Instead, cathepsin D, a soluble pepstatin-sensitive aspartyl endopeptidase, has been identified as the major enzyme which initiates insulin degradation in liver endosomes (Authier *et al*, 2002)

As in cultured cells exposed to insulin *in vitro* (Kasuga *et al,* 1981), liver insulin receptor expression and subcellular distribution are regulated by plasma insulin *in vivo*. Upon acute hyperinsulinemia, ligand-induced endocytosis of the receptor in liver is rapidly reversed, total receptor number remaining unchanged (Desbuquois *et al*, 1982). In contrast,

upon long lasting hyperinsulinemias, such as that observed in genetically obese Zucker rats, total cellular receptor number in liver is decreased while receptor number in endosomes is increased (Amessou *et al,* 2009). In Zucker rats, an increase in insulin receptor degradation accounts for the decrease in receptor expression (Amessou et al, 2009), as it does in isolated fibroblasts (Knutson, 1991b), and results in insulin resistance (Knutson *et al*, 1995). Ubiquitination of insulin receptor subunits by the E3 ubiquitin ligases c-Cbl (Ahmed *et al,* 2000), MG53 (Song *et al*, 2013) and March1 (Nagarajan*et al,* 2015), has been implicated in receptor degradation and inhibition of insulin signaling in liver and cultured cells. Unlike receptor ubiquitination by c-Cbl, which is induced by insulin, ubiquitination by March1 occurs in the basal state and results in a decrease in receptor expression at the cell surface. In the insulin-sensitive state, a decrease of March1 expression linked to inhibition of the transcription factor Foxo-1 results in an increased receptor expression. Some other negative regulators of insulin receptor expression are the adapter Grb10, which mediates ligand induced receptor ubiquitination and degradation (Ramos *et al*), and the β-secretase BACE-1, which cleaves the receptor ectodomain in the Golgi (Meakin *et al*, 2018)

As expected from the functional relationships between endocytosis and signaling (Sorkin & von Zastrow, 2009, von Zastrow & Sorkin, 2022), ligand-induced activation of the insulin receptor kinase and of downstream signaling pathways occurs both at the plasma membrane and in endosomes (reviewed by Baass *et al*, 1995, Bevan *et al,* 1996, and Bergeron *et al,* 1988, 1995, 2016). In both compartments, the activated receptor undergoes autophosphorylation at tyrosine residues (Khan *et al*, 1986, 1989) followed by dephosphorylation by phosphotyrosine phosphatases (Burgess *et al,* 1992, Faure *et al*, 1992, Drake *et al,* 1996, Li *et al*, 2006). Upon activation, the insulin receptor kinase recruits and phosphorylates a number of intracellular substrates that initiate discrete signaling pathways (reviewed by Siddle, 2011, 2012, Boucher *et al*, 2014, Saltiel, 2021). Major substrates are the

IRS and Shc proteins, which initiate the activation of the PI3K/Akt and Ras/Raf/Mek/Erk signaling pathways, respectively; the former pathway is preferentially activated at the plasma membrane, and the latter in endosomes. IRS, p85 PI3K and Akt signaling proteins recruited by the activated insulin receptor undergo redistribution between these cell compartments (Balbis *et al,* 2000, Drake *et al,* 2000). A selective activation of endosomal insulin receptor kinase mediates the *in vivo* hypoglycemic effect of bisperoxovanadium, a phosphotyrosine phosphatase inhibitor (Posner *et al,* 1994, Bevan *et al,* 1995). Several proteins recruited by the insulin receptor, such as PC-1/ENPP1 (Goldfine *et al*, 2008, Youngren, 2007), SOCS proteins (Ueki et al, 2004) and Grb7/10/14 adaptors (Holt and Siddle, 2005, Desbuquois *et al,* 2013) inhibit receptor autophosphorylation or receptor tyrosine kinase, whereas others, such as SH2B1/B2 adaptors are activators. The cell adhesion molecule CEACAM1, which upon association with the insulin receptor is phosphorylated by the receptor kinase, stimulates the endocytosis of the insulin-receptor complex (Najjar *et al,* 2002, 2018). In doing so, CEACAM1 regulates insulin sensitivity by promoting hepatic insulin clearance (Poy *et al,* 2002). Insulin receptors translocated to liver nuclei along with insulin signaling proteins associate with the transcriptional machinery at gene promoters and regulate the expression of insulin-inducible genes (Nelson *et al,* 2011, Sarfstein & Werner, 2013, Hancock *et al,* 2019).

In most previous studies, trafficking of insulin and its receptor in rat liver *in vivo* has been characterized using isolated plasma membrane and Golgi/endosome fractions, which account together for 15-20% of total receptor content. In the present study, these trafficking events have been revisited using analytical subcellular fractionation, with focus on distribution of [^{125}I]-insulin, native insulin and insulin receptor, physical characterization of the internalized receptor, and cell-free endosome to lysosome transfer of insulin and receptor.

Results and discussion

In vivo receptor-mediated uptake of [^{125}I]-insulin into rat liver

Based on the rate of plasma disappearance and volume of distribution of combined high and low affinity [^{125}I]-insulins, a receptor compartment with many properties of the receptor characterized *in vitro* has been identified *in vivo* in rabbits (Zeleznick & Roth, 1978). In subsequent studies, *in vivo* identification of insulin receptors in rat liver has been achieved by measurements of [^{125}I]-insulin uptake into the intact organ (Sodoyez *et al,* 1980) and isolated subcellular fractions (Izzo *et al,* 1979, 1983, Desbuquois *et al,* 1979, Posner *et al* 1980, Gagliardino *et al,* 1980, Papachristodoulou *et al,* 1981, Pease *et al*, 1985, 1987). Insulin uptake into intact liver has also been assessed by electron microscope autoradiography (Bergeron *et al,* 1977, 1979, Carpentier *et al*, 1979) and scintigraphic scanning (Sodoyez *et al,* 1983, 1985, Sodoyez-Goffaux *et al,* 1987, 1988) following injection of [^{125}I]- and [^{123}I]-labeled hormone, respectively. As expected from a specific and saturable receptor-mediated process, uptake of [^{125}I]-insulin was inhibited by excess co-injected native insulin but unaffected by unrelated hormones such as glucagon or growth hormone.

In agreement with a previous study (Posner *et al,* 1980), the ability of co-injected native insulin and insulin derivatives to inhibit uptake of [^{125}I]-insulin was dose-dependent and in correlation with their *in vitro* binding affinities for the insulin receptor. The dose of native insulin required for half-maximal inhibition of [^{125}I]-insulin uptake by a total liver particulate fraction was about 0.6 nmol, and des-alanine, des-asparagine insulin, proinsulin and des-octapeptide insulin were, respectively, 20%, 5% and 0.4% as potent as native insulin (supplementary Fig. 1).

Using an assay in which the *in vivo* uptake of injected [^{125}I]-insulin into rat tissues was compared to that of [^{125}I]-albumin, Whitcomb *et al* (1985) have shown that [^{125}I]-insulin

specific uptake was highest in liver. A similar observation has been made by Zeleznick and Roth (1978), who compared the *in vivo* uptake of high affinity chicken and low affinity guinea pig [^{125}I]-insulins into rabbit tissues. In agreement with these studies, the *in vivo* uptake of [^{125}I]-insulin into total particulate and microsomal fractions of rat tissues decreased in the order liver > adrenals > small intestine > lung > spleen > heart > adipose tissue > skeletal muscle (supplementary Fig. 2). As shown previously, kidney uptake of [^{125}I]-insulin was as high as liver uptake but was not saturable.

Subcellular distribution of [^{125}I]-insulin taken up by rat liver *in vivo*

Preparative subcellular fractionation procedures have shown that, upon *in vivo* uptake into rat liver, [^{125}I]-insulin is concentrated first at the plasma membrane and then in low density microsomal elements (Desbuquois *et al*, 1979, Posner *et al,* 1980). First proposed to originate from the Golgi apparatus, the latter were shown by the diaminobenzidine density shift procedure to be separable from the Golgi marker galactosyltransferase and hence identified as endosomes (Kay *et al,* 1984). On analytical subcellular fractionation, [^{125}I]-insulin taken up into liver was time-dependently concentrated in several components of different density: a single high-density component in the nuclear (N) fraction, and two components (of low and high density) in mitochondrial-lysosomal (ML) and microsomal (P) fractions (Bergeron *et al,* 1986). Based on the distribution of marker enzymes, the low density component in ML and P fractions was assigned to endosomes, and the high density component in N and P fractions to plasma membranes.

Using analytical subcellular fractionation, we also identified a single component of high density in the N fraction and two incompletely resolved components in the ML fraction (results not shown), but only a single component in the P fraction. On sucrose density gradients, this component was time-dependently shifted from the positions of *in vitro* insulin

binding activity and plasma membrane markers (peak density, about 1.16 g/ml) to those of galactosyltansferase and the mannose 6-phosphate/IGF-II receptor (peak density, 1.11-1.12 g/ml) (Fig 1). In agreement with previous studies (Pease *et al,* 1984, 1987), regardless of post-injection time digitonin treatment shifted the distribution of [^{125}I]-insulin towards higher densities, at the position of plasma membrane markers, while shifting to a lesser extent the distribution of galactosyltransferase (Fig. 2, left panels).

Although migrating in part at the position of lysosomal markers on density gradients (Bergeron *et al,* 1986), [^{125}I]-insulin taken up into liver was recovered to a limited extent in purified lysosomal fractions, even after treatment by chloroquine (Posner *et al,* 1982). Furthermore, insulin-containing structures present therein, which contained lipoprotein-like particles, were considered as non-lysosomal (Posner *et al,* 1982). We have previously suggested that the low association of internalized [^{125}I]-insulin with lysosomal fractions results from its rapid degradation in endosomes, resulting in the release of degradation products out of the endosomal lumen (Desbuquois *et al,* 1990, Chauvet *et al,* 1998). Accordingly, the distribution of [^{125}I]-insulin associated with the L fraction on Nycodenz density gradients has been examined and compared to that of [^{125}I]-proinsulin, which upon *in vivo* uptake into liver is degraded more slowly than insulin (Desbuquois *et al,* 2003), and of [^{125}I]-biotinylated insulin, the α amino group of which is blocked. As shown on Fig. 3, the migration of the two latter polypeptides towards high densities, at the position of lysosomal markers, was markedly increased at 8 min and 16 min post injection relative to that of [^{125}I]-insulin. These observations suggest that the low association of [^{125}I]-insulin with the high density region of the gradient results mainly from its rapid endosomal degradation.

***In vivo* insulin-induced changes in the subcellular distribution of the insulin receptor and of acid-extractable insulin in the microsomal fraction**

We have previously shown that following injection of a high dose of native insulin to rats, *in vitro* insulin binding activity rapidly increases along with insulin content in Golgi/endosome fractions, while simultaneously decreasing in the plasma membrane fraction (Desbuquois *et al*, 1982). In later studies, these time-dependent changes of insulin binding activity and insulin content in Golgi/endosome fractions of insulin-injected rats have been confirmed and shown to be increased by chloroquine treatment (Khan *et al,* 1985, Desbuquois *et al,* 1992). In the present study, the insulin-induced changes in receptor and ligand distribution have been reexamined using analytical subcellular fractionation

The distribution of *in vitro* insulin binding activity and immunoreactive insulin in primary subcellular fractions was first examined (Fig. 4). In control rats, insulin binding activity was recovered mainly in the nuclear (N) and microsomal (P) fractions (about 30% and 65% of total activity, respectively). Following injection of a saturating dose of insulin, a time-dependent decrease in insulin binding activity in the N fraction and a reciprocal increase of activity in the P fraction were observed. These changes were detectable at 2 min, achieved maximum at 30 min and were later slowly reversed. Injection of insulin also led to a rapid increase of immunoreactive acid-extractable hormone in N and P fractions (about 3 and 60 ng insulin per g liver, respectively), followed by a slow, time-dependent decrease (half-life, about 30 min).

The distribution of *in vitro* insulin binding activity and extractable insulin in the microsomal fraction on sucrose density gradients was then examined (Fig. 5 and Table 1). In control rats, the distribution of insulin binding activity largely overlapped that of the plasma membrane markers 5'nucleotidase and alkaline phosphodiesterase (median density, 1.155

g/ml). Injection of insulin led to a time-dependent shift of insulin binding activity towards lower densities, which achieved a maximum at 15-30 min and was nearly reversed at 2 h. At 15 min, the density distribution of activity was similar to those of galactosyltransferase and the IGF2/mannose 6 phosphate receptor (median density, 1.115 g/ml). As shown above for [^{125}I]-insulin distribution, digitonin treatment of the microsomal fraction shifted the distribution of insulin binding activity on sucrose gradients towards higher densities (median density, 1.179 g/ml) (Fig 2, right panels).

The time-dependent changes in the density distribution of acid-extractable insulin following insulin treatment paralleled those of insulin binding activity, but unlike the latter were not reversed after 30 min (Fig 5). Fractionation of light microsomal components (density < 1.15 g/ml) on self-generated Percoll density gradients showed that, up to 60 min after injection, insulin binding activity was recovered at low density, as was galactosyltransferase (Fig. 6). In contrast, the distribution of immunoreactive insulin on Percoll gradients was time-dependently shifted from low to high density, overlapping at late time the position of the lysosomal marker N-acetyl-β-D-glucosaminidase. Similar time-dependent changes in the distribution of [^{125}I]-insulin in Golgi/endosome fractions subjected to Percoll density gradients have been observed in untreated and chloroquine-treated rats (Khan *et al*, 1982, 1985). In addition, insulin receptors in lysosomal fractions have been localized on Percoll gradients in a vesicle of intermediate density between Golgi/endosomes and lysosomes (Khan *et al,* 1981).

The reversal of insulin-induced changes in insulin receptor distribution, along with the lack of change of total receptor number, suggests that upon acute ligand-induced endocytosis, internalized insulin receptors are fully recycled. However, these results do not exclude the possibility that the late restoration of receptor expression at the cell surface involves in part the synthesis of new receptors. To address this issue, the insulin-induced changes in receptor

distribution on sucrose density gradients were examined for sensitivity to *in vivo* treatment with cycloheximide, a protein synthesis inhibitor shown to inhibit insulin receptor synthesis in cultured cells (Knutson *et al*, 1985). As shown on Fig. 7, although *in vitro* insulin binding activity in the microsomal fraction equilibrated at lower densities in cycloheximide treated rats than in control animals, the early insulin-induced shift of activity towards lower densities (at 8 min) and its late reversal (at 3 h) were similar in both groups of rats. Cycloheximide treatment also affected neither the early insulin-induced decrease in insulin binding activity nor its late reversal in the plasma membrane. Finally, the time-dependent translocation of [^{125}I]-insulin in the microsomal fraction from high to low density was similar in cycloheximide-treated and untreated rats. Taken together, these observations suggest that following acute insulin-induced endocytosis, internalized insulin receptors are mainly if not fully recycled to the cell surface. In addition, they are consistent with the lack of effect on cycloheximide on the recycling of internalized photoaffinity radiolabeled insulin receptors in hepatocytes (Carpentier *et al*, 1986). As cycloheximide treatment, colchicine treatment of rats did not affect ligand-induced receptor endocytosis and little affected receptor recycling (Postel-Vinay *et al*, 1987).

Physical characterization of the insulin receptor in liver subcellular fractions

The observations described above suggest that, upon ligand-induced endocytosis, the insulin receptor retains functional and presumably structural integrity. To confirm this, the α and β subunits of the receptor in subcellular fractions of control and insulin-injected rats have been characterized by SDS-PAGE in association with affinity crosslinking (α subunit) and Western immunoblotting (both subunits).

As shown in many previous reports, a major insulin binding protein of about 130 kDa (expected Mw for the α subunit) was identified by affinity crosslinking in plasma membrane

and Golgi/endosome fractions incubated with [^{125}I]-insulin, and was also detectable, albeit to a lesser abundance, in lysosomal fractions (supplementary Fig. 3). An insulin binding protein of 120 kDa, previously identified as a proteolytic product of the α subunit generated *in vitro* but not *in vivo* (Lipson *et al,* 1986, 1988, Sanchez-Casas *et al,* 1995) was also detectable in plasma membranes. As shown previously, the generation of this 120 kDa protein did not occur at 4° C and was inhibited by PMSF, leupeptin and benzamidine.

When the centrifugation step after crosslinking was omitted, two additional proteins, of about 70 and 85 kDa, were detected; the 85 kDa protein bound specifically [^{125}I]-insulin, albeit with low affinity (supplementary Fig. 3) To address the possibility that these proteins were proteolytic fragments of the α subunit generated upon receptor endocytosis, subcellular fractions isolated shortly after *in vivo* injection of [^{125}I]-insulin were subjected to affinity crosslinking and SDS PAGE analysis (supplementary Fig. 4). As expected from the rapid degradation of internalized [^{125}I]-insulin, the expression of the crosslinked 130 kDa protein time-dependently decreased, whereas that of the 70 kDa protein concurrently increased. Further characterization of these proteins after Sephacryl S-300 gel filtration of solubilized endosomal extracts showed that, under nonreducing conditions, the 70 kDa protein was resolved into two components of about 60-65 and 50-55 kDa, respectively.

Although a 55 kDa proteolytic fragment of the insulin receptor has been shown to contain the major crosslinked binding site (Waugh *et al,* 1989), the 70 kDa protein identified under reducing conditions was probably unrelated to the 130 kDa protein (α subunit). Indeed, unlike the latter, it was not immunoprecipitated by two insulin receptor antibodies, did not bind to wheat germ agglutinin and showed no change in electrophoretic mobility following N-glycosidase treatment (results not shown). In addition, its molecular size differed from that of cathepsin D, a 45 kDa soluble aspartic acid protease involved in early steps of insulin

degradation in liver endosomes (Authier *et al,* 2002). On the other hand, the molecular size of this protein was closer to that of Hsp 72/73, a heart shock protein identified in cultured fetal hepatocytes (Zachayus *et al*, 1996). The latter protein has been shown to associate with the insulin receptor on co-immunoprecipitation and with [^{125}I]-insulin on affinity labeling.

On Western immunoblotting using an antibody against the C-terminal sequence 1336-1355 of the β subunit, a single or major protein of 95 kDa (expected molecular mass for the β subunit) was identified in plasma membrane, Golgi/endosome and lysosome fractions, confirming previous observations (supplementary Fig. 5). As anticipated, on Sephacryl gel filtration of solubilized fractions this 95 kDa protein was co-eluted with insulin binding activity. Two additional minor proteins of lower molecular mass (70-75 and 50-55 kDa), presumably proteolytic fragments of the β subunit, were also detectable in lysosomal fractions, with highest expression in the absence of protease inhibitors.

On Western immunoblotting using an antibody against the 542-551 sequence of the α subunit, two proteins of about 110-115 and 120-125 kDa were identified in the Golgi/endosome fraction and one protein of 140-150 kDa in the plasma membrane fraction (supplementary Fig. 6). As the 95 kDa protein (receptor β subunit), these proteins were also co-eluted with insulin binding activity on Sephacryl gel filtration. Multiple proteins of lower molecular weight (40-110 kDa) were also detected in plasma membrane and lysosomal fractions. Whether the 110-140 kDa proteins mentioned above are related to the α subunit of the insulin receptor is questionable. Indeed, autoradiographic signals were unaffected by the addition of excess 542-551 peptide (results not shown), and their electrophoretic mobility differed from that of the α subunit identified by affinity crosslinking.

Previous studies (Burgess *et al*, 1992, Desbuquois *et al,* 2008) have shown that, as expected from ligand-induced endocytosis of the insulin receptor, the expression of the 95

kDa protein (β subunit) following insulin injection rapidly decreases at the plasma membrane while increasing in endosomes, with a maximum at 15-30 min. Similar insulin-induced changes in the expression of the 135 kDa protein (α subunit) on affinity crosslinking in liver plasma membranes and endosomes have been reported (Sanchez Casas *et al*, 1995). The present study confirms the insulin-induced changes in the expression of the 95 kDa protein in cell fractions and shows that this protein does not undergo proteolysis during redistribution (supplementary Fig. 5). Unexpectedly, the expression of the 120 and 130 kDa proteins identified with the antibody against the α subunit 542-551 sequence in endosomes decreased instead of increasing after insulin injection (supplementary Fig. 6). Although unlikely, association of insulin to this sequence may have resulted in a loss of its accessibility to antibody.

Cell-free endosome to lysosome transfer of insulin and its receptor

Based on distribution on Nycodenz density gradients and release from lysosomal fractions by lysosome-disrupting drugs, [^{125}I]-insulin taken up by rat liver *in vivo* has been shown to undergo a partial transfer from endosomes to lysosomes in a cell-free system (Chauvet *et al*, 1998). So did, and to a greater extent owing to reduced endosomal degradation, [^{125}I]-proinsulin (Desbuquois *et al,* 2003). A partial endosome to lysosome transfer of insulin binding activity and receptor β subunit expression also occurred following injection of native insulin (Chauvet *at al,* 1998) and super-active insulin analogs (Authier *et al,* 2004). In the present study, the cell-free transfer of insulin and its receptor has been reexamined using purified endosomal and lysosomal fractions instead of the crude post-mitochondrial supernatant used previously.

Following injection of [^{125}I]-insulin, endosomal fractions were isolated and incubated with lysosomal L1 or L2 fractions and cytosol of untreated rats, the concentration of

lysosomal protein being varied relative to that of endosomal protein. The distribution of [^{125}I]-insulin on Nycodenz density gradients was then examined and compared to that of the lysosomal marker N-acetyl-β–D-glucosaminidase. At 4°C, at least 90% of [^{125}I]-insulin was recovered at the endosomal position (densities 1.08-1.10 g/ml), and less than 5% at the lysosomal position (density 1.12-1.14 g/ml). After incubation for 10 min at 37°C, [^{125}I]-insulin was in part transferred from the endosomal to the lysosomal position (Figs 8 and 9) However, as the ratio of lysosomal to endosomal protein decreased, the density at which [^{125}I]-insulin co-migrated with N-acetyl-β-D-glucosaminidase also decreased, whereas the amount of [^{125}I]-insulin recovered at the lysosomal position increased, with comparable results for L1 (Fig. 8) and L2 (Fig. 9) fractions. These observations suggest the formation of hybrid organelles of intermediate density between that of endosomes and that of lysosomes.

To assess whether the endosome to lysosome transfer of [^{125}I]-insulin involves a fusion of these organelles with content mixing, a cell-free assay exploiting the avidin-biotin interaction developed by Mullock *et al* (1994) was used. Endosomes isolated after injection of [^{125}I]-biotinylated insulin were incubated with lysosomes isolated after injection of avidin conjugated to galBSA and cytosol, following which the distribution of [^{125}I]-biotinylated insulin on Nycodenz density gradients was examined. In a first series of experiments, transfer of [^{125}I]-biotinylated insulin to lysosomes isolated after injection of avidin conjugated to galBSA was compared to transfer of [^{125}I]-insulin to lysosomes of control rats. Consistent with the *in vivo* studies described above, in this cell-free system [^{125}I]-biotinylated insulin was time-dependently transferred from the endosomal to the lysosomal position to a greater extent than [^{125}I]-insulin (Fig. 10). In a second series of experiments, the association of [^{125}I]-biotinylated insulin with avidin galBSA conjugate during incubation was assessed by immunoprecipitation using anti-avidin antibody. As shown on Fig. 10, while time dependently decreasing in the absence of biocytin or native biotinylated insulin, association of

[^{125}I]-biotinylated insulin to avidin increased in the presence of these agents. At 10 min, about 3% of total immunoprecipitated [^{125}I]-biotinylated insulin (no biocytin present) was bound to avidin in the presence of biocytin.

To confirm that the insulin receptor undergoes endosome to lysosome transfer along with insulin under cell-free conditions, endosomal and lysosomal fractions of rats which had been injected with native insulin were mixed and incubated at 37°C in the presence of cytosol. Following centrifugation on Nycodenz gradients, both low density (endosomal) and high density (lysosomal) components were collected and assayed for *in vitro* insulin binding activity and immunoreactive insulin content (Fig. 10). In incubation mixtures left at 4°C, about 14% of insulin binding activity and 18% of immunoreactive insulin were recovered at the lysosomal position. After incubation for 10 min at 37°C, in addition to a 50% decrease of insulin resulting from its endosomal degradation, insulin binding activity and insulin recovered at the lysosomal position were increased by 40% and 55%, respectively. As shown previously (Chauvet *et al*, 1998), in this cell free system an endosome to lysosome transfer of insulin receptor α subunit accompanied the transfer of insulin binding activity (Fig. 10). However, although decreased in the endosomal component, the expression of insulin receptor β subunit did not increase in the lysosomal component, probably as a result of degradation by lysosomal proteases.

Summary and conclusions

Using density gradients calibrated with markers for cell organelles, we have confirmed that, upon receptor-mediated uptake in rat liver, [^{125}I]-insulin undergoes rapid translocation from the plasma membrane to endosomes, with little further translocation to lysosomes. This intracellular pathway differs from that of proteins such as epidermal growth factor and asialoglycoproteins, which upon uptake into liver are in part transferred from endosomes to

lysosomes. However, owing to a reduced endosomal degradation, [^{125}I]-proinsulin associated to a greater extent than [^{125}I]-insulin with lysosomes, as did [^{125}I]-biotinylated insulin, the α amino group of which is blocked.

We have also confirmed that, following injection of native insulin, both insulin and its receptor in liver are rapidly translocated from the plasma membrane to endosomes. However, whereas at late times the internalized receptor was recycled to the plasma membrane, internalized insulin time-dependently segregated from the receptor and associated with endosomal components of higher density enriched in acid phosphatase. Neither receptor and insulin endocytosis, nor receptor recycling were affected by cycloheximide, an inhibitor of protein synthesis.

Using affinity crosslinking and Western immunoblotting procedures, we have confirmed that α and β subunits of the insulin receptor in liver subcellular fractions are expressed as proteins of about 135 kDa and 95 kDa, respectively. Following insulin treatment, the β subunit as detected by Western immunoblotting was rapidly translocated from the plasma membranes to endosomes. The 70 kDa insulin binding protein identified by affinity crosslinking in endosomes was probably unrelated to the receptor α subunit.

A time-dependent endosome to lysosome transfer of *in vivo* internalized [^{125}I]-insulin and [^{125}]-biotinylated insulin occurred in a liver cell-free system. As shown previously for the transfer of [^{125}I]-asialofetuin (Mullock *et al*, l989), the transfer of [^{125}I]-insulin was function of the abundance of lysosomes relative to that of endosomes. Upon cell-free transfer from endosomes to lysosomes loaded with avidin galBSA conjugate, [^{125}I]-biotinylated insulin was in part immunoprecipitated by anti-avidin antibody, consistent with endosome to lysosome fusion with organelle content mixing. However, association of [^{125}]-biotinylated insulin with avidin galBSA conjugate was lower than reported for association of endosomal avidin-

asialofetuin with lysosomal [^{125}I]-biotinylated polymeric IgA (Mullock *et al*, 1994, 1998). This may have resulted from a more rapid degradation of [^{125}I]-biotinylated insulin, as compared to that of [^{125}I]-biotinylated polymeric IgA.

Experimental procedures

Materials

Porcine insulin and recombinant human insulin were purchased from Novo Nordisk. Porcine proinsulin, des-alanine des-asparagine insulin and des-octapeptide insulin were gifts from Eli Lilly Research laboratories. Biotinylated insulin, avidin, N-succinimidyl 3-(2-pyridyldithio)propionate (SPDP), protein A, cycloheximide, and antibodies against insulin and avidin were from Sigma-Aldrich. Antibodies against the β subunit of the insulin receptor were from Santa Cruz Biotechnology. Antibodies against partial sequences of α (542-551) and β (1336-1355) subunits of the human insulin receptor were gifts of Drs Emmanuel Van Obberghen and Daniel Lane, respectively. Nitrocellulose membranes were from Biorad. Other chemicals were obtained commercially as described previously.

Preparation of galBSA and conjugation of galBSA to avidin

GalBSA was prepared from bovine serum-albumin by reductive lactosamination as described by Wilson (1978). Conjugation of galBSA to avidin was performed using SPDP as described by Carllson *et al* (1978). Briefly, 8 mg (0.12 μmol) of galBSA diluted into 1.8 ml of 0.1 M phosphate buffer, pH 7, 0.1 M NaCl, was reacted with 0.3 mg (0.93 μmol) of SPDP dissolved into 30 μl of ethanol. After 30 min at room temperature, the reaction mixture was dialyzed against 500 ml of 0.1 M acetate buffer, pH 4.5, 0.1 M NaCl. Based on measurements of absorbance at 280 and 343 nm after addition of 50 μl of 50 mM

dithiothreitol (DTT), the number of SPDP groups introduced into galBSA was estimated as about 7 per molecule. Reaction of avidin (5,4 mg, 0.08 μmol) with SPDP (0,15 mg, 0.46 μmol) was carried out n a similar manner. Following reduction by DTT, thiol-containing gal BSA was coupled to avidin-2-pyridyl disulphide by thiol-disulfide exchange. After 20 h at 23°C, the reaction mixture was subjected to gel filtration on Sephacryl S300. About 70% of total applied protein as measured by absorbance at 280 nm was eluted ahead of BSA (66 kDa), close to the elution position of alcohol dehydrogenase (150 kDa).

Preparation of [^{125}I]-labeled polypeptides.

[^{125}I]-labeled insulin, biotinylated insulin and proinsulin (400-600 Ci/mmol) were prepared using lactoperoxidase and purified by gel-filtration on Sephadex G50. As shown in a previous study (Desbuquois *et al,* 2003), iodination of insulin occurred mainly (70%) at tyrosine A14. [^{125}I]-labeled protein A was prepared and purified in a similar manner.

Animal experiments.

In vivo procedures were approved by the French institutional committee for use and care of experimental animals. Male Sprague Dawley rats (body weight, 200 g), obtained from Charles River France and Elevage Janvier, were fasted for 16 h prior to experiments. Native insulin, insulin derivatives and proinsulin, [^{125}I| labeled insulin and biotinylated insulin (2-5 pmol each) and avidin conjugated to galBSA were diluted into 0.5 ml of physiological saline and injected into the penis vein under ether or Nembutal anesthesia. When indicated rats injected with native and [^{125}I]-labeled insulin received an intraperitoneal injection of cycloheximide (0.8 mg per 100 g of body weight) 3 h prior to injection. At the indicated

times, the liver was removed and immediately homogenized in 0.25 M sucrose.

Liver subcellular fractionation

This was performed using preparative and analytical and preparative procedures as described previously (Desbuquois *et al*, 1979, Posner *et al,* 1980, Bergeron *et al,* 1986). Nuclear (N), mitochondrial-lysosomal (ML), light mitochondrial (L) and microsomal (P) fractions were prepared from liver homogenates by differential centrifugation. In analytical procedures, these primary fractions were quantitatively further fractionated by centrifugation on linear sucrose (N, ML and P fractions) and Nycodenz (L fraction) density gradients. When indicated the microsomal fraction was treated by digitonin (0.17%) for 30 min prior to density gradient subfractionation. Sucrose gradients (density range, 1.04-1.25 g/ml) were centrifuged for 15 h at 27,000 rpm in a Beckman SW 28 rotor, and Nycodenz gradients (density range, 1.04-1.16 g/ml) for 1 h at 30.000 rpm in a Beckman SW41 rotor. About 15-20 fractions were collected and assayed for density by refractometry. Low density (d < 1.15 g/ml) microsomal subfractions were further fractionated in a Percoll density gradient (32% Percoll in 0.25 M sucrose) generated by centrifugation for 30 min at 30,000 rpm in a Beckman 50Ti rotor. Purified plasma membranes were isolated from the N fraction according to Hubbard *et al* (1983), Golgi-endosomal fractions from the P fraction according to Ehrenreich *et al* (1973), and lysosomal L1 and L2 fractions from the L fraction according to Wattiaux *et al* (1978).

Subcellular fractions isolated after injection of [^{125}I]-labeled insulin, biotinylated insulin and proinsulin were analyzed for radioactivity, and fractions isolated from control and insulin-injected rats for *in vitro* insulin binding activity and acid-extractable insulin content as described previously (Desbuquois *et al,* 1982, 2003). The distribution of these components on sucrose and Nycodenz density gradients was compared to that of markers for plasma membranes (5'nucleotidase and alkaline phosphodiesterase), Golgi (galactosyltransferase), endosomes (IGF2/mannose 6-phosphate receptor) and lysosomes (acid phosphatase and N-acetyl β-D-glucosaminidase). Median densities for enzymes, [^{125}I]-insulin, *in vitro* insulin

binding activity and immunoreactive insulin in the P fraction are shown in Table 1, and representative distributions of several enzymes and insulin binding activity in supplementary Fig. 8.

Physical characterization of insulin receptor subunits in liver cell fractions.

The α subunit of the insulin receptor was characterized by cross-linking to *in vitro* added or *in vivo* injected [^{125}I]-insulin with DSS followed by SDS PAGE and autoradiography. Both subunits were also analyzed by Western immunoblotting with antibodies against sequences 542-551 (α subunit) and 1336-1355 (β subunit) of the human insulin receptor. When indicated insulin receptor crosslinked to [^{125}I]-insulin was characterized after gel filtration of Triton X-100 solubilized fractions on Sephacryl S-300. [^{125}I]-labeled protein A was used to reveal immune complexes in Western blots. In some experiments, a commercial goat polyclonal antibody against insulin receptor β subunit was used and immune complexes were revealed by enhanced chemiluminescence detection.

Endosome to lysosome transfer of *in vivo* internalized [^{125}I]-insulin, [^{125}I]-biotinylated insulin, native insulin and insulin receptor in a cell-free system

Liver Golgi/endosome fractions of rats sacrificed 8 min after injection of [^{125}I]-insulin were incubated with lysosomal and cytosolic fractions of control rats in 0.5-1 ml of 0.25 M sucrose/5 mM TES containing 1 mM ATP, 5 mM $MgCl_2$, 5 mM phosphocreatine and 0.5 mg/ml creatine kinase. After 5-20 min at 37°C, incubation mixtures were cooled to 4°C and centrifuged on linear Nycodenz gradients (density range, 1.04-1.16 g/ml) calibrated with the lysosomal enzyme N-acetyl β-D-glucosaminidase. Endosome to lysosome transfer of [^{125}I]-biotinylated insulin was studied in a similar manner but in this case lysosomal fractions were isolated 30 min after injection of avidin conjugated to galBSA. Association of [^{125}I]-biotinylated insulin loaded endosomes with avidin-galBSA loaded lysosomes was assessed

using a content mixing assay as described by Mullock *et al* (1994). Briefly, after incubation in presence of native biotinylated insulin (10 μg/ml) or biocytin (0,2 mg/ml), incubation mixtures were diluted into 50 mM Tris buffer, pH 7.5, containing 1% Triton X-100 and protease inhibitors (PMSF 1 mM, benzamidine 1 mM, bacitracin 1 mg/m1, 1,10 phenanthroline 5 mM, pepstatin 1 μM). Following incubation of the lysed mixtures with anti-avidin antibody at 4°C for 24 h, protein A-Sepharose was added and immunoprecipitated [^{125}I]-biotinylated insulin was determined. It was expressed as % of the total mmunoprecipitated in the absence of biotinyl blocking agents.

Measurement of insulin concentration and insulin binding activity in liver subcellular fractions.

The concentration of insulin in acid extracts of liver subcellular fractions was measured by radioimmunoassay using [^{125}I]-insulin and anti-insulin antibody. Insulin binding activity in Triton X-100 solubilized subcellular fractions was measured using [^{125}I]-insulin as ligand and polyethyleneglycol to precipitate insulin-receptor complexes. Both assays have been described previously (Desbuquois *et al*, 1982, 2003).

Author contribution

Khadija Tahiri has been involved in the physical characterization of the insulin receptor in liver subcellular fractions; Françoise Fouque, in the biochemical characterization of these fractions; and Marie-Catherine Postel-Vinay, in the study of the effect of cycloheximide on [^{125}I]-insulin and insulin receptor trafficking. Bernard Desbuquois coordinated these studies and wrote the manuscript.

Aknowledgments

The authors gratefully acknowledge the technical assistance of Brigitte de Gallé, Henriette Burlet and Aline Dupuis.

This work is dedicated to the memory of Geneviève Chauvet, who carried out the studies on the cell-free endosome to lysosome transfer of insulin and its receptor.

References

Ahmed Z, Smith BJ, Pillay TS (2000). The APS adapter protein couples the insulin receptor to the phosphorylation of c-Cbl and facilitates ligand-stimulated ubiquitination of the insulin receptor. *FEBS Lett* 475, 31-4

Amessou M, Tahiri K, Chauvet G, Desbuquois B (2010). Age-related changes in insulin receptor mRNA and protein expression in genetically obese Zucker rats. *Diabetes Metab* 36, 120-128.

Authier F, Rachubinski RA, Posner BI, Bergeron JJ (1994a). Endosomal proteolysis of insulin by an acidic thiol metalloprotease unrelated to insulin degrading enzyme. *J Biol Chem.* 269, 3010-3016.

Authier F, Posner BI, Bergeron JJ. (1994b). Hepatic endosomes are a major physiological locus of insulin and glucagon degradation in vivo. *Cellular Proteolytic Systems*, 89-113.

Authier F, Posner BI, Bergeron JJ. (1995a). Insulin-degrading enzyme. *Clin Invest Med.* 19, 149-160.

Authier F, Bergeron JJ, Ou WJ, Rachubinski RA, Posner BI, Walton PA. (1995b). Degradation of the cleaved leader peptide of thiolase by a peroxisomal proteinase. *Proc Natl Acad Sci U S A.* 92(9), 3859-63.

Authier F, Danielsen GM, Kouach M, Briand G, Chauvet G (2001). Identification of insulin domains important for binding to and degradation by endosomal acidic insulinase. *Endocrinology* 142, 276-285.

Authier F, Metioui M, Fabrega S, Kouach M, Briand G (2002). Endosomal proteolysis of internalized insulin at the C-terminal region of the B chain by cathepsins D. *J Biol Chem* 277, 9437-46.

Authier F, Merlen C, Amessou M, Danielsen GM (2004). Use of high affinity insulin analogs to assess the functional relationships between insulin receptor trafficking, mitogenic signaling and mRNA expression in rat liver. *Biochimie* 86, 157-166.

Balbis A, Baquiran G, Bergeron JJ, Posner BI. (2000). Compartmentalization and insulin-induced translocations of insulin receptor substrates, phosphatidylinositol 3-kinase, and protein kinase B in rat liver. *Endocrinology*, 141, 4041-9.

Baass PC, Di Guglielmo GM, Authier F, Posner BI, Bergeron JJ (1995). Compartmentalized signal transduction by receptor tyrosine kinases. *Trends Cell Biol* 5,465-70.

Berg T, Gjoen T, Bakke O (1995). Physiological functions of endosomal proteolysis. *Biochem J* 307, 313-325

Bergeron JJM, Evans WH, Geschwind II (1973a). Insulin binding to rat liver Golgi fractions. *J Cell Biol* 59, 771-776.

Bergeron JJ, Ehrenreich JH, Siekevitz P, Palade GE. (1973b). Golgi fractions prepared from rat liver homogenates. II. Biochemical characterization. *J Cell Biol* 59, 73-88.

Bergeron JJ, Levine G, Sikstrom R, O'Shaughnessy D, Kopriwa B, Nadler NJ, Posner BI. (1977). Polypeptide hormone binding sites in vivo: initial localization of 125I-labeled insulin to hepatocytes as visualized by electron microscope radio autography. *Proc Natl Acad Sci USA.* 74, 5051-5.

Bergeron JJ, Sikstrom R, Hand AR, Posner BI (1979). Binding and uptake of 125I-insulin into rat liver hepatocytes and endothelium. An in vivo radioautographic study. *J Cell Biol* 80, 427-430.

Bergeron JJ, Searle N, Khan MN, Posner BI. (1986). Differential and analytical subfractionation of rat liver components internalizing insulin and prolactin. *Biochemistry* 25, 1756-64.

Bergeron JJ, Lai WH, Kay DG, Doherty JJ, Khan MN, Posner BI (1988). The endosomal apparatus and transmembrane signaling. *Adv Exp Med Biol* 234, 213-224.

Bergeron JJ, Di Guglielmo GM, Baass PC, Authier F, Posner BI (1995). Endosomes, receptor tyrosine kinases internalization and signal transduction. *Biosci Rep* 15, 411-418.

Bergeron JJ, Di Guglielmo GM, Dahan S, Dominguez M, Posner BI. (2016). Spatial and Temporal Regulation of Receptor Tyrosine Kinase Activation and Intracellular Signal Transduction. *Annu Rev Biochem* 85, 573-97.

Bevan AP, Burgess JW, Drake PG, Shaver A, Bergeron JJ, Posner BI (1995a). Selective activation of the rat hepatic endosomal insulin receptor kinase. Role for the endosome in insulin signaling. *J Biol Chem* 270, 10784-91.

Bevan AP, Drake PG, Yale JF, Shaver A, Posner BI (1995b). Peroxovanadium compounds: biological action and mechanism of insulin mimesis. *Mol Cell Biochem* 153, 49-58

Bevan AP, Drake PG, Bergeron JJ, Posner BI (1996). Intracellular signal transduction: the tole of endosomes. *Trends Endocrinol Metab* 7, 13-21.

Bevan AP, Krook A, Tikerpae J, Seabright PJ, Siddle K, Smith GD. (1997). Chloroquine extends the lifetime of the activated insulin receptor in endosomes. *J Biol Chem.* 272, 26833-40.

Bevan AP, Seabright PJ, Tikerpae J, Posner BI, Smith GD, Siddle K. (2000). The role of insulin dissociation from its endosomal receptor in insulin degradation. *Mol Cell Endocrinol* 164, 145-57.

Boucher J, Kleinridders A, Kahn CR (2014). Insulin receptor signaling in normal and insulin-resistant states. *Cold Spring Harb Perspect Biol* 6 : a 009191.

Burgess JW, Wada I, Ling N, Khan MN, Bergeron JJ, Posner BI (1992). Devrease in beta-subunnit phosphotyrosine content correlates with internalization and activation of the endosomal insulin receptor kinase. *J Biol Chem* 267, 10077-10086.

Carlsson J, Drevin H, Axen R (1978). Protein thiolation and reversible protein-protein conjugation. N-succinimidyl 3-(2-pyridyldithio) propionate, a new heterobifunctional reagent. *Biochem J* 173, 723-737.

Carpentier JL, Gorden P, Barrazone P, Freychet P, Le Cam A, Orci L (1979. Intracellular localization of 125I-labeled insulin in hepatocytes from intact rat liver. *Proc Natl Acad Sci USA* 76, 2803-2807.°

Carpentier JL, Gazzano H, Van Obberghen E, Fehlmann M, Freychet P, Orci L. (1986). Intracellular pathway followed by the insulin receptor covalently coupled to 125I-photoreactive insulin during internalization and recycling. *J Cell Biol*. 1986, 102(3):989-96.

Chauvet G, Tahiri K, Authier F, Desbuquois B. (1998). Endosome-lysosome transfer of insulin and glucagon in a liver cell-free system. *Eur J Biochem.* 254, 27-37.

Chen Y, Huang C, Qi X, Chen C (2019). Insulin receptor trafficking : consequences for insulin sensitivity and diabetes. *Int J Mol Sci* 20, 5007.

Clot JP, Janicot M, Fouque F, Desbuquois B, Haumont PY, Lederer F. (1990). Characterization of insulin degradation products generated in liver endosomes: in vivo and in vitro studies. *Mol Cell Endocrinol.* 72, 175-85.

Cuatrecasas P, Desbuquois B, Krug F (1971). Insulin-receptor interactions in liver cell membranes. *Biochem Biophys Res Commun*. 44 :333-9.

Cuatrecasas P. (1972). Properties of the insulin receptor isolated from liver and fat cell membranes. *J Biol Chem.* 247, 1980-91.

Desbuquois B, Willeput J, Huet de Froberville A. (1979). Receptor-mediated internalisation of insulin in intact rat liver. A biochemical study. *FEBS Lett*. 106(2):338-4

Desbuquois B, Lopez S, Burlet H. (1982). Ligand-induced translocation of insulin receptors in intact rat liver. *J Biol Chem*. 257(18):10852-60.

Desbuquois B, Janicot M, Dupuis A. (1990). Degradation of insulin in isolated liver endosomes is functionally linked to ATP-dependent endosomal acidification. *Eur J Biochem.* 193, 501-12.

Desbuquois B, López S, Janicot M, Burlet H, de Gallé B, Fouque F. (1992). Role of acidic subcellular compartments in the degradation of internalized insulin and in the recycling of the internalized insulin receptor in liver cells: in vivo and in vitro studies. *Diabete Metab*.18, 104-12.

Desbuquois B, Chauvet G, Kouach M, Authier F. (2003). Cell itinerary and metabolic fate of proinsulin in rat liver: in vivo and in vitro studies. *Endocrinology*, 144, 5308-21

Desbuquois B, Béréziat V, Authier F, Girard J, Burnol AF (2008). Compartmentalization and in vivo insulin-induced translocation of the insulin-signaling inhibitor Grb14 in rat liver. *FEBS J.* 275, 4363-77

Desbuquois B, Carré N, Burnol AF (2013). Regulation of insulin and type 1 insulin-like growth factor signaling and action by the Grb10/14 and SH2B1/B2 adaptor proteins. *FEBS J* 280(3):794-816.

Doherty JJ 2nd, Kay DG, Lai WH, Posner BI, Bergeron JJ. (1990). Selective degradation of insulin within rat liver endosomes. *J Cell Biol*. 110, 35-42.

Drake PG, Balbis A, Wu J, Bergeron JJ, Posner BI. (2000). Association of phosphatidyl inositol 3-kinase with the insulin receptor: compartmentation in rat liver. *Am J Physiol Endocrinol Metab* 279, E266-74.

Drake PG, Bevan AP, Burgess JW, Bergeron JJ, Posner BI. (1996). A role for tyrosine phosphorylation in both activation and inhibition of the insulin receptor tyrosine kinase in vivo. *Endocrinology* 137, 4960-8.

Duckworth WC (1988). Insulin degradation: mechanisms, products and significance. *Endocr Rev,* 9(3), 319-345.

Duckworth WC, Bennett RG, Hamel FG (1998). Insulin degradation: progress and potential. *Endocr Rev* 19 (5), 608-624.

Freychet P, Roth J, Neville DM Jr. (1971). Insulin receptors in the liver: specific binding of 125I insulin to the plasma membrane and its relation to insulin bioactivity. *Proc Natl Acad Sci U* S A. 68, 1833-7.

Gagliardino JJ, Pessacq MT, Turyn D, Dellacha JM (1980. Insulin binding to liver cells: a simple and useful in vivo model. *Horm Metab Res* 12, 300-3.

Gletsu NA, Field CJ, Clandinin MJ (1999). Obese mice have higher insulin receptor levels in the hepatocyte cell nucleus following insulin stimulation in vivo with an oral glucose meal. *Biochim Biophys Acta* 1454, 251-260

Goldfine ID, Smith GJ (1976). Binding of insulin to isolated nuclei. *Proc Natl Acad Sci USA* 73, 1427-1431.

Goldfine ID, Maddux BA, Youngren JF, Reaven G, Accili D, Trischitta V, Vigneri D, Frittitta L (2008). The Role of Membrane Glycoprotein Plasma Cell Antigen 1/Ectonucleotide Pyrophosphatase Phosphodiesterase 1 in the Pathogenesis of Insulin Resistance and Related Abnormalities. *Endocr Rev* 29, 62-75.

Hall C, Yu H, Choi E (2020). Insulin receptor endocytosis in the pathophysiology of insulin resistance. *Exp Mol Med* 52, 911-920

Hamel FG, Posner BI, Bergeron JJ, Frank BH, Duckworth WC. (1988). Isolation of insulin degradation products from endosomes derived from intact rat liver. *J Biol Chem.* 263, 6703-

Hamel FG, Mahoney MJ, Duckworth WC. (1991). Degradation of intraendosomal insulin by insulin-degrading enzyme without acidification. *Diabetes* 40, 436-443.

Hancock ML, Meyer RC, Mistry M, Khetani RS, Wagschai A, Shin T, Ho Sui SJ, Naar AM, Flanagan JG (2019). Insulin receptor associates with promoters genome-wide and regulate gene expression. *Cell* 177, 722-736.

Holt LJ, Siddle K (2005). Grb10 and Grb14: enigmatic regulators of insulin action – and more ? *Biochem J*. 388, 393-406.

Hubbard AL, Wall DA, Ma A. (1983). Isolation of rat hepatocyte plasma membranes. I. Presence of the three major dins. *J Cell Biol.* 96, 217-29.

Iraburu MJ, Garner T, Montiel-Duarte C. (2021). Revisiting endosomal trafficking under insulin receptor activation. *Int J Mol Sci* 22, 6978.

Izzo JL, Roncone AM, Helton DL, Izzo MJ. (1979). Subcellular distribution of intraportally injected 125I-insulin in rat liver. *Arch Biochem Biophys.* 198, 97-109.

Izzo JL Sr, Roncone AM, Kleiman F. (1983). Subcellular distribution of 125-insulin by rat liver: specificity and regulatory factors. *Am J Physiol.* 244, E272-81.

Kasuga M, Kahn CR, Hedo JA, Van Obberghen E, Yamada KM (1981). Insulin-induced receptor loss in cultured human lymphocytes is due to accelerated receptor degradation. *Proc Natl Acad Sci USA* 78, 6917-21.

Kay DG, Khan MN, Posner BI, Bergeron JJ. (1984). In vivo uptake of insulin into hepatic Golgi fractions: application of the diaminobenzidine-shift protocol. *Biochem Biophys Res Commun*.23(3):1144-8.

Kesten D, Horovitz-Fried M, Brutman-Barazani T, Sampson SR (2018). Insulin-induced translocation of IR to the nucleus in insulin responsive cells requires a nuclear translocation sequence. *Biochim Biophys Acta , Mol Cell Res1865*(4), 551-559.

Khan MN, Posner BI, Verma AK, Khan RJ, Bergeron JJ. (1981). Intracellular hormone receptors: evidence for insulin and lactogen receptors in a unique vesicle sedimenting in lysosome fractions of rat liver. *Proc Natl Acad Sci U S A*. 78(8):4980-4.

Khan,MN, Posner BI, Khan RJ, Bergeron JJ. (1982). Internalization of insulin into rat liver Golgi elements. Evidence for vesicle heterogeneity and the path of intracellular processing. *J Biol Chem.* 257

Khan MN, Savoie S, Khan RJ, Bergeron JJ, Posner BI. (1985). Insulin and insulin receptor uptake into rat liver. Chloroquine action on receptor recycling. *Diabetes* 34, 1025-30.

Khan MN, Savoie S, Bergeron JJ, Posner BI (1986). Characterization of rat liver endosomal fractions. In vivo activation of insulin-stimulable receptor kinase in these structures. *J Biol Chem.* 261, 8462-72.

Khan MN, Baquiran G, Brule C, Burgess J, Foster B, Bergeron JJ, Posner BI. (1989). Internalization and activation of the rat liver insulin receptor kinase in vivo. *J Biol Chem.264,* 12931-40.

Knutson VP, Ronnett GV, Lane MD (1985). The effects if cycloheximide and chloroquine on insulin receptor metabolism. Differential effects on receptor recycling and inactivation and insulin degradation. *J Biol Chem.* 260, 14180-88.

Knutson VP (1991a). Cellular trafficking and processing of the insulin receptor. *FASEB J.* 5, 2130-2138.

Knutson VP (1991b). Proteolytic processing of the insulin receptor β subunit is associated with insulin-induced receptor down-regulation. *J Biol Chem.* 266, 15656-15662.

Knutson VP, Donnelly PV, Balba, Y, Lopez-Reyes M. (1995). Insulin resistance is mediated by a proteolytic fragment of the insulin receptor. *J Biol Chem*. 270, 24972-24981.

Leissring MA (2021). Insulin-degrading enzyme: paradoxes and possibilities (2021). *Cells* 10, 2445.

Leissring MA, Gonzalez-Casimiro CM, Merino B, Suire CN, Perdomo G (2021). Targeting insulin-degrading enzyme in insulin clearance. *Int J Mol Sci* 22, 2235.

Li C, Baquiran G, Gu F, Tremblay ML, Fazel A, Bergeron JJ, Posner BI. (2006). Insulin receptor kinase-associated phosphotyrosine phosphatases in hepatic endosomes: assessing the role of phosphotyrosine phosphatase-1B. *Endocrinology*, 147, 912-8.

Lipson KE, Kolhatkar AA, Donner DB. (1988). Cell surface proteolysis and down-regulation of the hepatic insulin receptor. Evidence for selective sorting of intact and degraded receptors after internalization. *J Biol Chem.* 263, 10495-501.

Lipson, KE, Kolhatkar AA, Donner DB. (1989). Insulin stimulates proteolysis of the α-subunit, but not the β-subunit, of its receptor at the cell surface in rat liver. *Biochem J.* 261, 333-340.

Meakin PJ, Mezzapesa A, Benabou E, Haas ME, Bonardo B, Grino M, Brunel JM, Desbois-Mouthon C, Biddinger SB, Govers R, Ashford MLJ, Peiretti F (2018). The beta-secretase BACE1 regulates the expression of the insulin receptor in the liver. *Nat Commun* 9, 1306

Morcavallo A, Stefanello M, Iozzo RV, Belfiore A, Morrione A (2914). Ligand-mediated endocytosis and trafficking of the insulin-like growth factor receptor I and insulin receptor modulate receptor function. *Front Endocrinol* 17, 5, 220

Mullock BM, Branch WJ, van Schaik M, Gilbert M, Luzio JP (1989). Reconstitution of an endosome-lysosome interaction in a cell-free system**.** *J Cell Biol* 108, 2093-2099**.**

Mullock BM, Perez JH, Kuwana T, Gray SR, Luzio JP (1994). Lysosomes can fuse with a late endosomal compartment in a cell-free system from rat liver. *J Cell Biol* 126, 1173-1182.

Mullock BM, Bright NA, Fearon CW, Gray SR, Luzio JP (1998). Fusion of lysosomes with late endosomes produces a hybrid organelle of intermediate density and is NSF dependent. *J Cell Biol* 140, 591-601.

Nagarajan A, Petersen MC, Nasiri AR, Butrico G, Fung A, Ruan HB, Kursawe R, Caprio S, Thibodeau J, Bourgeois-Daigneault MC, Sun L, Gao G, Bhanot S, Jurczak MJ, Green MR, Shulman GI, Wajapeyee N (2016). March1 regulates insulin sensitivity by controlling cell surface insulin receptor levels. *Nat Commun.* 31, 12639

Najjar SM (2002). Regulation of insulin action by CEACAM1. *Trends Endocrinol Metab* 13, 240-245.

Najjar SM, Perdomo G (2019). Hepatic insulin clearance: mechanism and physiology. *Physiology* 34, 198-215.

Nelson JD, LeBoeuf RC, Bomsztyk K (2011). Direct recruitment of insulin receptor and ERK signaling cascades to insulin-inducible gene loci. *Diabetes* 60, 127-137.

Olefsky J, Johnson J, Liu F, Edwards P, Baur S (1975). Comparison of 125-I-insulin binding and degradation in isolated rat hepatocytes and liver membranes. *Diabetes* 24, 801-810.

Papachristodoulou DK, Birbeck MS, Scott GS, Thomas JH. (1981). Subcellular distribution of intravenously injected 125I-labeled insulin in rat liver. *Int J Biochem.* 13, 293-301.

Pease RJ, Sharp GA, Smith GD, Peters TJ. (1984). Isolation and partial characterization of the rat liver ligandosome fraction. *Biochim Biophys Acta* 774, 56-66.

Pease RJ, Smith GD, Peters TJ. (1985). Degradation of endocytosed insulin in rat liver is mediated by low-density vesicles. *Biochem J.* 228, 137-46.

Pease RJ, Smith GD, Peters TJ. (1987). Characterization of insulin degradation by rat-liver low-density vesicles. *Eur J Biochem.*164, 251-7.

Peavy DE, Hamel FG, Kincke VL, Duckworth WC. (1985). Evidence that bacitracin alters intracellular insulin metabolism in isolated rat hepatocytes. *Diabetes* 34, 217-21.

Petersen MC, Shulman GI. (2018). Mechanisms of insulin action and insulin resistance. *Physiol Rev*. 98, 2133-2223.

Podlecki DA, Smith RM, Kao M, Tsai P, Hueksteadt T, Brandenburg D, Lasher RS, Jarett L, Olefsky JM (1987). Nuclear translocation of the insulin receptor. A possible mediator of insulin's long term effects. *J Biol Chem*. 262, 3362-8.

Posner BI, Josefsberg Z, Bergeron JJ. (1978). Intracellular polypeptide hormone receptors. Characterization of insulin binding sites in Golgi fractions from the liver of female rats. *J Biol Chem.* 253, 4067-73

Posner BI, Patel B, Verma AK, Bergeron JJ. (1980). Uptake of insulin by plasmalemma and Golgi subcellular fractions of rat liver. *J Biol Chem*. 255, 735-41.

Posner BI, Patel BA, Khan MN, Bergeron JJ. (1982). Effect of chloroquine on the internalization of 125I-insulin into subcellular fractions of rat liver. Evidence for an effect of chloroquine on Golgi elements. *J Biol Chem.* 257, 5789-99.

Posner BI, Faure R, Burgess JW, Bevan AP, Lachance D, Zhang-Sun G, Fantus IG, Ng JB, Hall DA, Lum BS, *et al* (1994). Peroxovanadium compounds. A new class of potent phosphotyrosine phosphatase inhibitors which are insulin mimetics. *J Biol Chem* 269, 4596-604.

Postel-Vinay MC, Kayser C, Desbuquois B. (1987). Ligand-induced changes in the subcellular distribution of insulin receptors in rat liver: effects of colchicine. *Mol Cell Endocrinol*. 52, 199-204.

Poy, MN, Yang Y, Rezaei K, Fernström MA, Lee AD, Kido Y, Erickson SK, Najjar SM (2002). CEACAM1 regulates insulin clearance in liver. *Nat Genet* 30, 270-276.

Ramos FJ, Langlais PR, Hu D, Dong LQ, Liu F (2006). Grb10 mediates insulin-stimulated degradation of the insulin receptor: a mechanism of negative regulation. *Am J Physiol* (*Endocrinol Metab*) 290, E1262-6

Sánchez-Casas P, Yusta B, Blázquez E. (1995). Insulin-induced proteolysis of the insulin receptor alpha-subunit does not occur in vivo but is prevented in vitro by proteinase inhibitors. *Eur J Biochem* 232, 747-54.

Sarfstein R, Werber H. (2013). Nuclear insulin and insulin-like growth factor-1 receptors: a novel paradigm in signal transduction. *Endocrinology* I54, 1672-9.

Seabright PJ, Smith GD. (1996). The characterization of endosomal insulin degradation intermediates and their sequence of production. *Biochem J.* 320, 947-56.

Siddle K (2011). Signaling by insulin and IGF receptors: supporting acts and new players. *J Mol Endocr* 47, R1-R10.

Siddle K (2012). Molecular basis of signaling specificity of insulin and IGF receptors: neglected corners and recent advances. *Front Endocrinol* 3, 34, 1-24.

Smith GD, Peters TJ (1982). The localization in rat liver of alkaline phosphodiesterase to a discrete organelle implicated in ligand internalization. *Biochim Biophys Acta* 716, 24-30.

Smith GD, Christensen JR, Rideout JM, Peters TJ (1989). Hepatic processing of insulin. Characterization of differential inhibition by weak bases. *Eur J Biochem* 181, 287-294.

Sodoyez JC, Sodoyez-Goffaux FR, Morris YM. (1980). ^{125}I-insulin: kinetics of interaction with its receptors and rate of degradation in vivo. *Am J Physiol*. 239 (*Endocrinol Metab* 2), E3-E11.

Sodoyez JC, Sodoyez-Goffaux F, Guillaume M, Merchie G. (1983). [125I] insulin metabolism in normal rats and humans: external detection by a scintillation camera. *Science,* 219, 865-867.

Sodoyez JC, Sodoyez-Goffaux F, von Frenckell R, De Vos CJ, Treves S, Kahn CR. (1985). Differing effects of anti-insulin serum and anti-insulin receptor serum on ^{123}I-insulin metabolism in rats. *J Clin Invest.* 75, 1455-1462.

Sodoyez-Goffaux F, Sodoyez JC, Koch M, Dozio N, Arquilla ER, McDougall B, De Vos CJ, von Frenckell R. (1987). Scintigraphic distribution of complexes of anti-insulin antibodies and ^{123}I-insulin. In vivo studies in rats. *J Clin Invest.* 80, 466-74.

Sodoyez-Goffaux F, Sodoyez JC, Koch M, De Vos CJ, Frank BH. (1988). Scintigraphic distribution of 123 I labelled proinsulin, split conversion intermediates and insulin in rats *Diabetologia* 31, 848-854.

Song R *et al* (2013). Central role of E3 ubiquitin ligase MG53 in insulin resistance and metabolic disorders. *Nature* 494, 375-379.

Sorkin A, von Zastrow M (2009). Endocytosis and signaling: intertwining molecular networks. *Nat Rev Mol Cell Biol* 10, 609-622.

Terris S, Steiner DF (1975). Binding and degradation of 125I-insulin by rat hepatocytes. *J Biol Chem*. 250, 8389-98.

Ueki K, Kondo T, Kahn CR (2004). Suppressor of cytokine signaling 1 (SOCS-1) and SOCS-3 cause insulin resistance through inhibition of tyrosine phosphorylation of insulin receptor substrate proteins by discrete mechanisms. *Mol Cell Biol* 24, 5434-5446.

Vigneri R, Goldfine ID, Wong KY, Smith GJ, Pezzino V. J(1978). The nuclear envelope. The major site of insulin binding in rat liver nuclei. *J Biol Chem* 253, 2098-103.

Villa-Pérez P, Merino B, Fernández-Díaz CM, Cidad P, Lobatón CD, Moreno A, Muturi HT, Ghadieh HE, Najjar SM, Leissring MA, Cózar-Castellano I, Perdomo G (2018). Liver-specific ablation of insulin-degrading enzyme causes hepatic insulin resistance and glucose intolerance, without affecting insulin clearance in mice. *Metabolism* 88, 1-11.

Von Zastrow N, Sorkin A (2021). Mechanisms for regulating and organizing receptor signaling by endocytosis. *Annu Rev Biochem,* 90, 709-737.

Wattiaux R, Wattiaux-De Coninck S, Ronveaux-Dupal LF, Dubois F (1978). Isolation of rat liver lysosomes by isopycnic centrifugation in a metrizamide gradient. *J Cell Biol* 78, 349-68.

Waugh SM, DiBella EE, Pilch PF (1989). Isolation of the insulin receptor containing the major site of cross-linking binding. *Biochemistry* 28, 3448-3455.

Whitcomb DC, O'Dorisio TM, Cataland S, Shetzline MA, Nishikawara MT. (1985). Identification of tissue insulin receptors: use of a unique in vivo radioreceptor assay. *Am J Physiol* 249 (*Endocrinol Metab* 12), E561-E567.

Wong KY, Hawley D, Vigneri R, Goldfine ID (1988). Comparison of solubilized and purified plasma membrane and nuclear insulin receptors. *Biochemistry* 27, 375-9.

Youngren JF (2007). Regulation of insulin receptor function. *Cell Mol Life Sci* 64, 873-891.

Zachayus JL, Benatmane S, Plas C. (1996). Role of Hsp70 synthesis in the fate of the insulin-receptor complex after heat shock in cultured fetal hepatocytes. *J Cell Biochem*. 61, 216-29.

Zeleznik AJ, Roth J. (1978). Demonstration of the insulin receptor in vivo in rabbits and its possible role as a reservoir for the plasma hormone. *J Clin Invest* 21, 1363-1374.

Table 1. Median densities for distribution of protein, marker enzymes, [^{125}I]-labeled and native insulin, and insulin binding activity in the microsomal fraction. Liver microsomal fractions isolated from untreated rats and from animals sacrificed after injection of [^{125}I]-labeled and native insulin were subjected to sucrose density gradient centrifugation as described in Experimental Procedures. When indicated microsomal fractions were treated by digitonin. About 20 subfractions were collected and assayed for the components indicated. Median densities, expressed as g/ml (mean ± SEM of the indicated number of determinations) were calculated from distributions as a function of density.

Protein, insulin binding activity and marker enzymes

	Untreated	Digitonin-treated
Protein	1.164 ± 0.002 (6)	
In vitro insulin binding	1.166 ± 0.002 (5)	1.181 ± 0.003 (
5'Nucleotidase	1.156 ± 0.003 (3)	1.184 ± 0.002 (4)
Alkaline phosphodiesterase	1.168 ± 0.002 (2)	1.189 ± 0.002 (4)
Glucose 6-phosphatase	1.206	
Acid phosphatase	1.177 ± 0.006 (3)	
N-acetyl-β-D-glucosaminidase	1.200 ± 0.005	1.142 ± 0.002 (3)
Galactosyltransferase	1.125 ± 0.001(3)	1.153 ± 0.006 (4)
IGF2/M6P receptor	1. 127 ± 0.002 (7)	

***In vivo* [^{125}I]-insulin uptake**

Time	Untreated*	Untreated	Digitonin-treated
30 sec	1.176 ± 0.002 (5)	1.164 ± 0.001 (2)	1.187 ± 0.001 (4)
90 sec	1.133 ± 0.002 (4)	1.132 ± 0.006 (2)	1.179 ± 0.004 (4)
4 min	1.123 ± 0.004 (7)	1.120 ± 0.002 (2)	1.178 ± 0.001 (4)
8 min	1.117 ± 0.004 ()	1.116 ± 0.004 (2)	1.171 ± 0.003 (4)
16 min		1.114	
24 min		1.112	

***In vitro* insulin binding activity and insulin content after insulin injection**

Time after injection	Insulin binding activity	Insulin content
0	1.155 ± 0.007 (6)	not determined
30 sec	1.147 ± 0.002 (2)	1.146 + 0.003 (2)
2 min	1.130 ± 0.006 (6)	1.127 + 0.005 (4)
5 min	1.126 ± 0.008 (3)	1.124 + 0.001 (2)
15 min	1.118 ± 0.005 (6)	1.118 + 0.002 (4)
30 min	1.116 ± 0.001 (2)	1.110
60 min	1.135 ± 0.008 (5)	1.114 + 0.006 (3)
120 min	1.141 ± 0.002 (2)	1.109 + 0.002 (2)

*In this series the microsomal fraction was layered below the density gradient

Figure legends

Figure 1. Density distribution of [^{125}I]-insulin taken up into the liver microsomal fraction *in vivo*. Microsomal fractions were isolated at the indicated time after injection of [^{125}I]-insulin and subjected to centrifugation on sucrose density gradient. The distribution of [^{125}I]-insulin at 20 sec (blue bars), 90 sec (red bars) and 5 min (grey bars) after injection has been plotted against normalized density intervals of 0.01 g/ml. The results shown are the mean of 5 determinations. Arrows indicate the peaks of galactosyltransferase (GTR), IGF2/mannose 6-phosphate receptor (IGF2/M6P), 5'nucleotidase (5'N) and alkaline phosphodiesterase (PDE)

Figure 2. Effect of digitonin treatment of the microsomal fraction on the density distribution of injected [^{125}I]-insulin and insulin receptor. Liver microsomal fractions were prepared at the indicated time after injection of [^{125}I]-insulin (left panels) or native insulin (right panels); control rats (right panels) were left untreated. Fractions were treated by digitonin (red bars) or left untreated (blue bars), following which the distribution of [^{125}I]-insulin (left panels) and of *in vitro* insulin binding activity (right panels) on sucrose density gradients was examined. Representative experiments (of three) are shown.

Figure 3. Comparative density distributions of [^{125}I]-labeled insulin, biotinylated insulin and proinsulin taken up into light mitochondrial (L) fractions *in vivo*. L fractions prepared at the indicated time after injection of [^{125}I]-labeled insulin, biotinylated insulin and proinsulin were sub-fractionated by centrifugation on linear Nycodenz density gradients (density range, 1.05 to 1.15 g/ml). Twenty subfractions were collected and assayed for radioactivity (blue bars, [^{125}I]-insulin; red bars, [^{125}I]-biotinylated insulin and [^{125}I]-proinsulin). The results shown are representative of two to three experiments. N-acetyl–β-D-glucoinidase activity was recovered in fractions 12-20.

Figure 4. *In vitro* insulin binding activity and insulin content of primary liver subcellular fractions isolated after insulin injection. Rats were sacrificed at the indicated time after injection of insulin (50 μg) or left untreated. Liver nuclear (N), mitochondrial-lysosomal (ML) and microsomal (P) fractions were prepared and assayed for *in vitro* insulin binding activity and extractable immunoreactive insulin content. The results shown are the mean ± SEM of three determinations.

Figure 5. Distribution on density gradients of insulin binding activity and insulin in liver microsomal fractions of control and insulin-treated rats. Microsomal fractions were isolated from rats killed at the indicated time after injection of native insulin (50 μg) or left untreated. Following centrifugation on sucrose density gradients, subfractions were collected and assayed for density, *in vitro* insulin binding activity and extractable immunoreactive insulin content, with results normalized to density intervals of 0.01 g/ml. The results shown are representative of at least three experiments. The positions of galactosyltransferase, 5'nucleotidase and alkaline phosphodiesterase peaks on the gradients (not shown) are the same as in Figure 1.

Figure 6. Distribution on Percoll density gradients of insulin binding activity and insulin in liver microsomal subfractions of control and insulin-treated rats. Microsomal subfractions (density < 1.15 g/ml) of rats killed at the indicated time after insulin injection were subjected to centrifugation on Percoll density gradients. Fifteen subfractions of increasing density were collected and assayed for insulin binding activity and extractable immunoreactive insulin content. The results shown are representative of three experiments. Galactosyl transferase was recovered mainly at low density (fractions 1-5) and acid phosphatase at high density (fractions 8-15).

Figure 7. Effect of *in vivo* cycloheximide treatment on the subcellular distribution of insulin binding activity in microsomal fractions of control and insulin-treated rats and of [^{125}I]-insulin taken up into liver *in vivo*. A, distribution on sucrose density gradients of insulin binding activity in microsomal fractions of control and insulin-injected rats (8 min and 3 h after injection of 0.3 mg insulin). B, median density of *in vitro* insulin binding activity at the indicated time after insulin injection. C, insulin binding activity in plasma membrane fractions of control and insulin-injected rats (300 μg) at the indicated time after injection. D, median densities of radioactivity in microsomal fractions isolated 30 sec and 4 min in after injection of [^{125}I]-insulin. The results shown are representative or the mean of three experiments.

Figure 8. Distribution of [^{125}I] insulin taken up into rat liver *in vivo* on density gradients upon cell-free endosome to lysosome transfer. Endosomal fractions isolated 8 min after injection of [^{125}I]-insulin were incubated with lysosomal L1 (left) and L2 (right) fractions and cytosol of control rats. The ratios of lysosomal to endosomal protein concentration were, respectively, 6,4 (A) and 0,8 (B) for the L1 fraction, and 7,6 (C) and 1,9 (D) for the L2 fraction. After 10 min at 4°C and 37°C, incubation mixtures were subjected to centrifugation on Nycodenz density gradients. Twenty fractions were collected and assayed for density, radioactivity and N-acetyl-β-D-glucosaminidase activity. Representative distribution profiles for radioactivity and enzyme activity are shown.

Figure 9. Determination of [^{125}I]-insulin migrating at the lysosomal position and of corresponding density as a function of lysosome abundance upon cell-free endosome to lysosome transfer. Endosomal fractions isolated after injection of [^{125}I]-insulin were incubated with lysosomal L1 (left) and L2 (right) fractions and cytosol of control rats as described in legend to figure 8. The percentage of [^{125}I]-insulin co-migrating with N-acetyl-

β-glucosaminidase (A) and the corresponding density (B) on Nycodenz density gradients have been plotted against the lysosomal to endosomal protein ratio.

Figure 10. Cell-free endosome to lysosome transfer of [^{125}]-biotinylated insulin taken up into rat liver *in vivo*. Liver endosomal fractions of rats isolated 8 min after injection of [^{125}I]-biotinylated insulin were mixed with lysosomal (L1 and L2) fractions isolated 30 min after injection of avidin-galBSA conjugate and cytosol. After incubation for 5, 10 and 20 min at 37°C, incubation mixtures were subjected to centrifugation on Nycodenz density gradients and to immunoprecipitation by anti-avidin antibody in the presence and absence of biocytin or native biotinylated insulin. In parallel experiments, endosome fractions of rats killed 8 min after injection of [^{125}I]-insulin were incubated with lysosomal and cytosolic fractions of untreated rats prior to density gradient centrifugation. A, comparative distributions of [^{125}I]-insulin and [^{125}I]-biotinylated insulin in cytosolic, endosomal and lysosomal gradient subfractions (density range, 1.05-1.07, 1.07-1.11 and 1.11-1.15 g/ml, respectively). B, [^{125}I]-biotinylated insulin immunoprecipitated by anti-avidin antibody in the absence and presence of biocytin, expressed as % of total in the medium and % immunoprecipitated in the absence of biocytin, respectively. C, cell-free endosome to lysosome transfer of [^{125}I]-insulin binding activity (left) and immunoreactive insulin (right). D, cell-free endosome to lysosome transfer of [^{125}I]-insulin binding activity (top), insulin receptor α subunit crosslinked to [^{125}I]-insulin (middle) and immunodetected β subunit (bottom).

Supplementary figures legends

Supplementary Fig. 1. Dose dependent inhibition of [^{125}I]-insulin binding to liver microsomal membranes by native insulin and related polypeptides. Native insulin, des-alanine des-asparagine insulin, des-octapeptide insulin and proinsulin were examined at the indicated concentrations for their ability to inhibit the *in vivo* uptake of [^{125}I]-insulin into liver microsomal fractions.

Supplementary Fig. 2. In vivo uptake of [^{125}I]-insulin by rat tissues. [^{125}I]-insulin, alone and with excess native insulin (50 μg), was injected to rats and examined for its ability to be taken up by the particulate fraction of the indicated tissues at 2 min post injection. Nonspecific uptake was determined after co-injection of [^{125}I]-inulin and excess native insulin.

Supplementary Fig. 3. SDS PAGE analysis of proteins crosslinked to *in vitro* added [^{125}I]-insulin. A, proteins identified in microsomal (P), plasma membrane (MP), Golgi/endosomal (GE) and lysosomal (L1 and L2) fractions. B, proteins identified in the plasma membrane fraction incubated with [^{125}I]-insulin for 10 min (1), 30 min (2), 60 min (3) and 120 min (4) in the absence of protease inhibitors (left), and for 2 h in the presence of 1 mM PMSF (a), 2 mg/ml bacitracin (b), 10 mg/ml leupeptin (c), 5 mM 1,10 phenantroline (d), 1 mM benzamidine (e) and 1 mM N-ethylmaleimide (f) (right). C, proteins identified in plasma membrane (MP) and Golgi/endosomal (GE) fractions incubated with [^{125}I]-insulin for 60 min at 4° C (a), and for 5 min (b), 15 min (c) and 1 h (d) at 30° C. D, [^{125}I]-labeled proteins identified in cell fractions that were not subjected to centrifugation. Left, proteins in Golgi/endosomal (GE) and lysosomal (L1 and L2) fractions in the absence (1) and presence (2) of excess native insulin. Right: proteins in the GE fraction in the absence (1) and presence of native insulin at concentrations of 0,04 (2), 0,2 (3), 1 (4) and 5 (5) μg/ml.

Supplementary Fig. 4. SDS PAGE analysis of proteins crosslinked to *in vivo* injected [^{125}I] insulin. A, proteins identified under reducing conditions in plasma membrane (MP) and Golgi/endosomal (GE) fractions isolated 2 min (a), 5 min (b) and 10 min (c) after injection of [^{125}I] insulin (left), and in the Golgi/endosomal (GE) fraction isolated at 10 min in the absence (c) and presence of injected chloroquine (d) and bacitracin (e) (right). Arrows indicate the position of the 135 kDa and 70 kDa [^{125}I]-labeled proteins. The determination of the radioactivity associated with these two proteins and of the total TCA-soluble radioactivity as a function of time is shown below. B, chromatographic elution profile and SDS PAGE analysis of endosomal proteins crosslinked to *in vivo* injected [^{125}I]-insulin. Proteins of a Golgi/endosomal fraction isolated 6 min after injection have been crosslinked to [^{125}I]-insulin, solubilized by Triton X-100 (0.33%) and subjected to chromatography on a Sephacryl S-300 column (1 x 50 cms) equilibrated in 0.1 M ammonium acetate buffer, pH 7.4, calibrated with molecular weight markers. Lower figure: elution pattern of the radioactivity showing two components (peak 1, fractions 16-22, and peak 2, fractions 32-35) eluted ahead of [^{125}I]-insulin (peak 3, fractions 40-60). Arrows indicate the elution positions of dextran blue (BD), thyroglobulin (TG, 669 kDa), apoferritin (AF, 443 kDa), alcohol dehydrogenase (AD), 150 kDa) and serum-albumin (SA, 66 kDa). Upper figures: SDS-PAGE analysis and autoradiography of eluate fractions showing, under reducing conditions (upper gel) a 135 kDa protein in peak 1 (fractions 19 and 20) and a 70 kDa protein in peak 2 (fractions 30-32), and under non-reducing conditions (lower gel), a protein of > 200 kDa in peak 1 (fractions 24-26) and two proteins, of about 65 and 50 kDa, in peak 2 (fractions 30-34). C, SDS PAGE analysis of ^{125}I-labeled proteins identified in peaks 1 and 2 of Sephacryl S-300 chromatographic eluates. Left and middle: proteins identified under nonreducing conditions following adsorption of eluates peaks 1 and 2 on WGA-Sepharose 6MB (lanes 1, precipitates; lanes 2, supernatants). Right: comparative migration profile, under nonreducing conditions,

of peak 2 endosomal protein cross-linked to [^{125}I]-insulin (lane 1), [^{125}I]-labeled serum-albumin (lane 2) and [^{125}I]-labeled heat shock protein (hsp) 70 (lane 3).

Supplementary Fig 5. Western blot analysis of proteins identified in liver subcellular fractions of control and insulin-injected rats using an antibody against insulin receptor β subunit. Left: lane 1, microsomal fraction of control rats; lanes 2 and 3, plasma membrane fraction of control (2) and insulin-treated (3) rats; lanes 4 and 5, Golgi/endosome fraction of control (4) and insulin-treated (5) rats; lanes 6-8, lysosomal L (6), L1 (7) and L2 (8) fractions of control rats. Right: plasma membrane (PM) and Golgi/endosomal (GE) fractions of control and insulin-injected rats at the indicated time after insulin injection

Supplementary Fig. 6. Western blot analysis of proteins identified in liver subcellular fractions of control and insulin-treated rats using an antibody against insulin receptor α subunit. Left: lane 1, microsomal fraction of control rats; lanes 2-4, plasma membrane fraction of control (2, 3) and insulin-treated (4) rats; lanes 5-7, Golgi/endosomal fraction of control (5) and insulin-treated (6, 7) rats; lanes 8-10, lysosomal L (8), L1 (9) andL2 (10) fractions of control rats. Right: plasma membrane (PM) and Golgi/endosomal (GE) fractions of control and insulin-injected rats at the indicated time after insulin injection.

Supplementary Fig. 7. Chromatographic elution profile of proteins immunodetected in liver plasma membrane and Golgi/endosome fractions. Plasma membrane (PM) and Golgi/endosome (GE) fractions have been subjected to gel filtration on a Sephacryl S-300 column (1 x 50 cms) after solubilization by Triton X-100. Initial (T) and eluate fractions (numbered 22-30) have been probed by Western immunoblotting using antibodies against the α (top) and β (bottom) subunits of the insulin receptor. Insulin binding activity as measured using [^{125}I]-insulin was recovered in eluate fractions 22-26.

Supplementary Fig. 8. Density distribution of enzymes and insulin receptor in the liver microsomal fraction. A microsomal fraction of control rats has been subjected to sucrose density gradient centrifugation, following which the distribution of galactosyltransferase (Gtr), IGF2/mannose 6-phosphate receptor (IG2/M6P), alkaline phosphodiesterase (PDE) and insulin receptor (IR) has been plotted against normalized density intervals of 0.01 g/ml. The results shown are representative of at least three separate experiments.

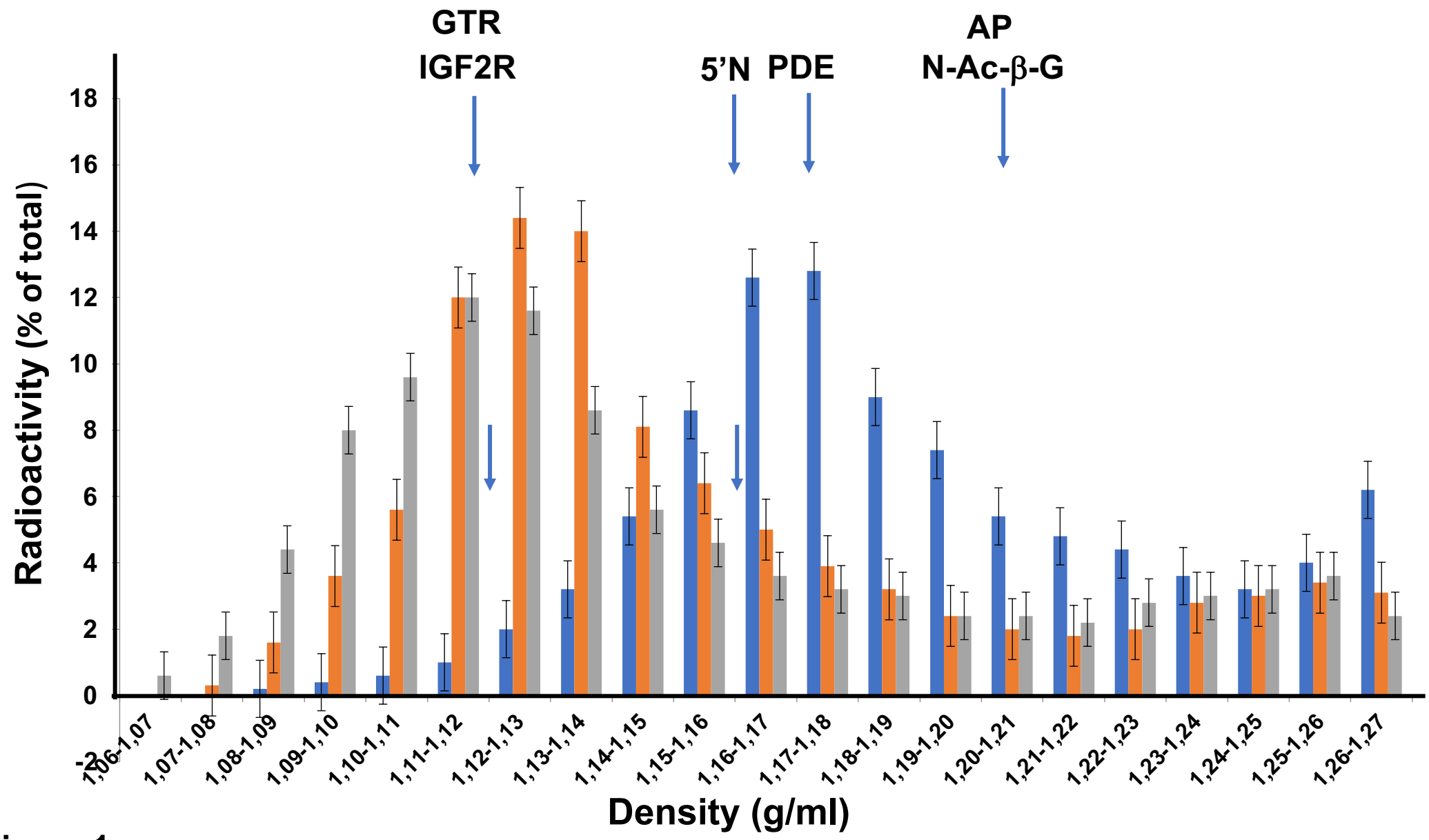
GTR
IGF2R
5'N
PDE
AP
N-Ac-β-G
Radioactivity (% of total)
18
16
14
12
10
8
6
4
2
0
-2
1,06-1,07
1,07-1,08
1,08-1,09
1,09-1,10
1,10-1,11
1,11-1,12
1,12-1,13
1,13-1,14
1,14-1,15
1,15-1,16
1,16-1,17
1,17-1,18
1,18-1,19
1,19-1,20
1,20-1,21
1,21-1,22
1,22-1,23
1,23-1,24
1,24-1,25
1,25-1,26
1,26-1,27
Density (g/ml)

Figure 1

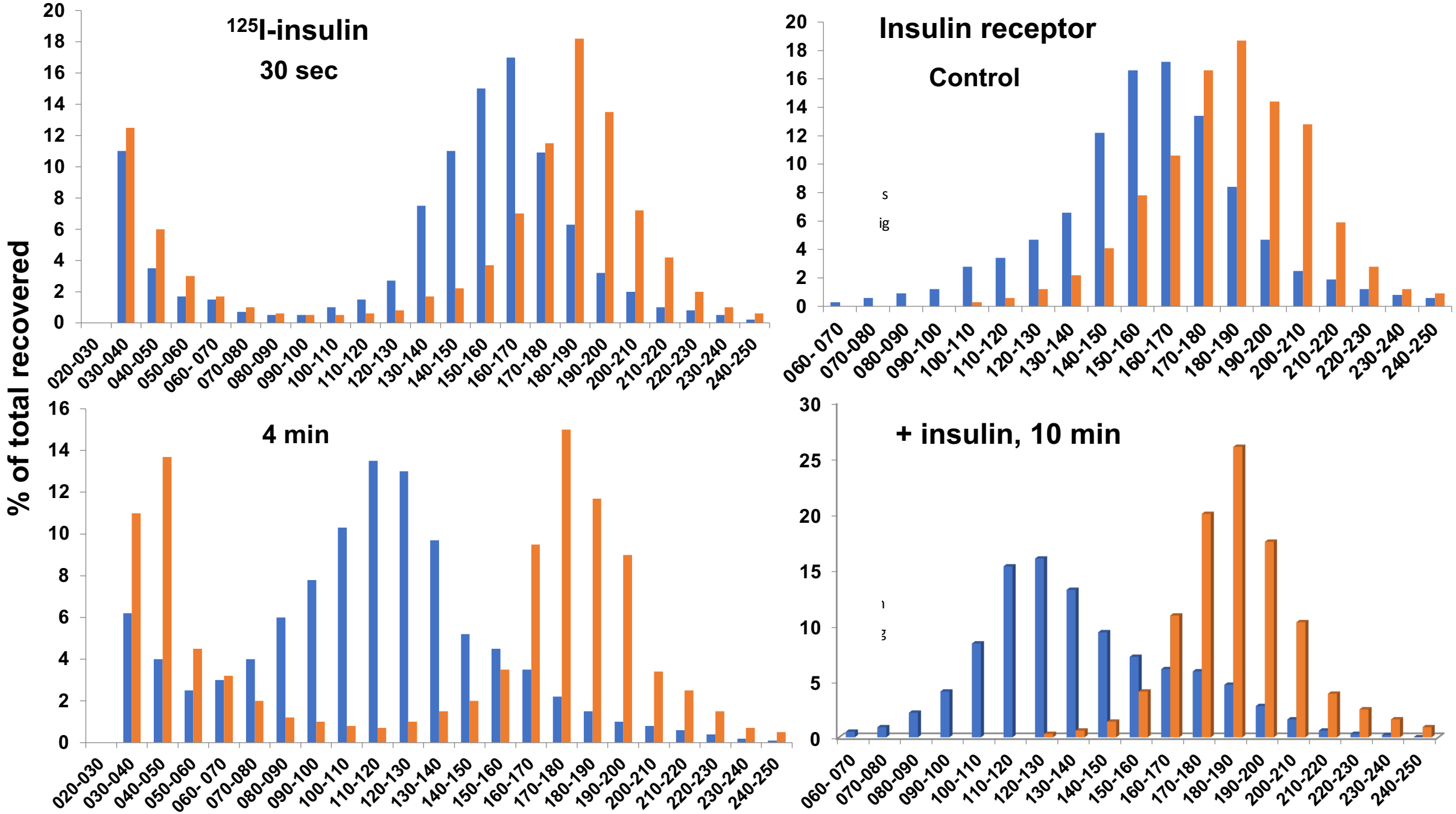
% of total recovered
125I-insulin
30 sec
Insulin receptor
Control
4 min
+ insulin, 10 min
020-030
030-040
040-050
050-060
060- 070
070-080
080-090
090-100
100-110
110-120
120-130
130-140
140-150
150-160
160-170
170-180
180-190
190-200
200-210
210-220
220-230
230-240
240-250
Density (g/ml - 1)

Figure 2

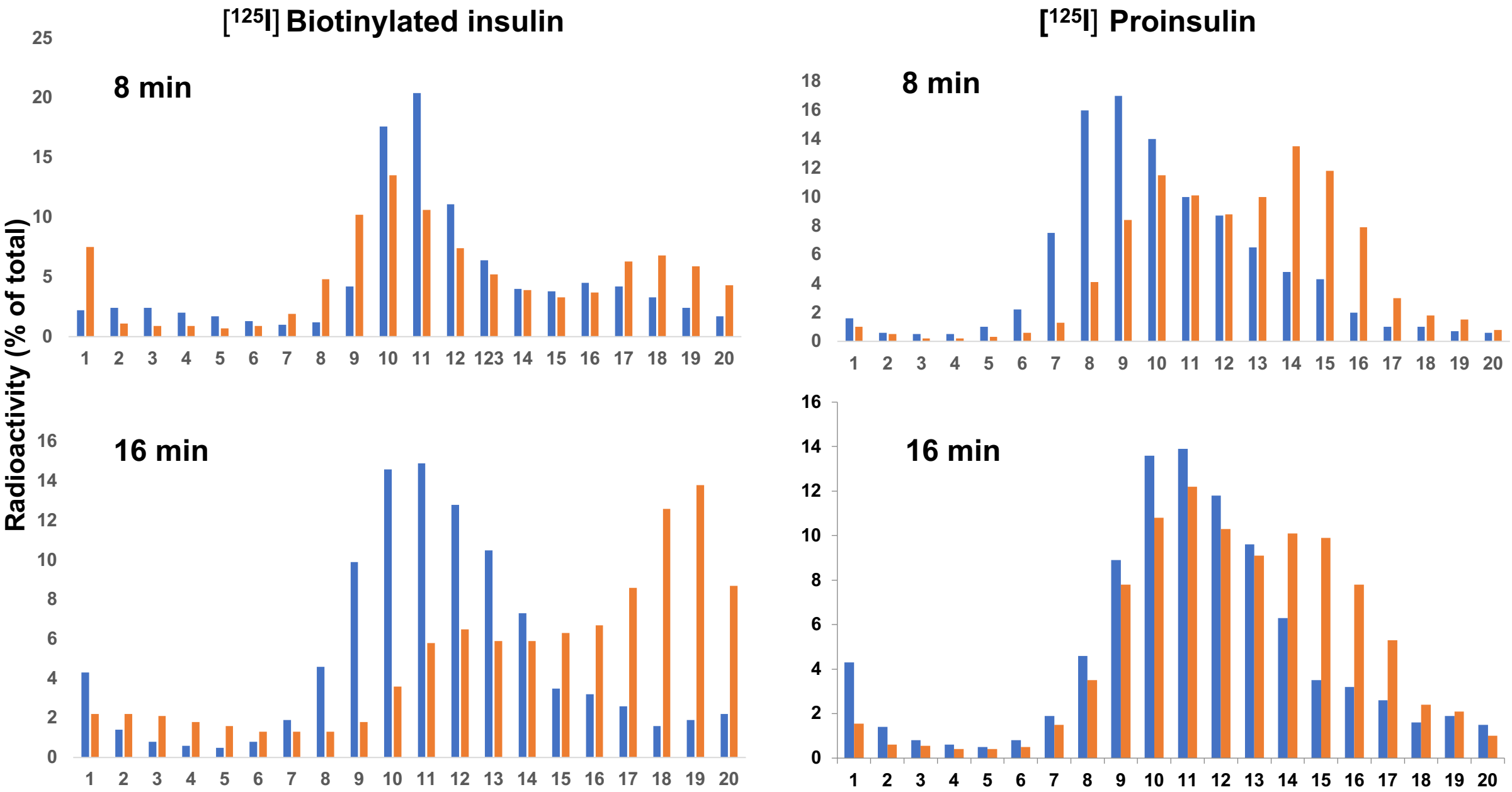
[125I] Biotinylated insulin
[125I] Proinsulin
8 min
8 min
16 min
16 min
Radioactivity (% of total)
Fraction number

Figure 3

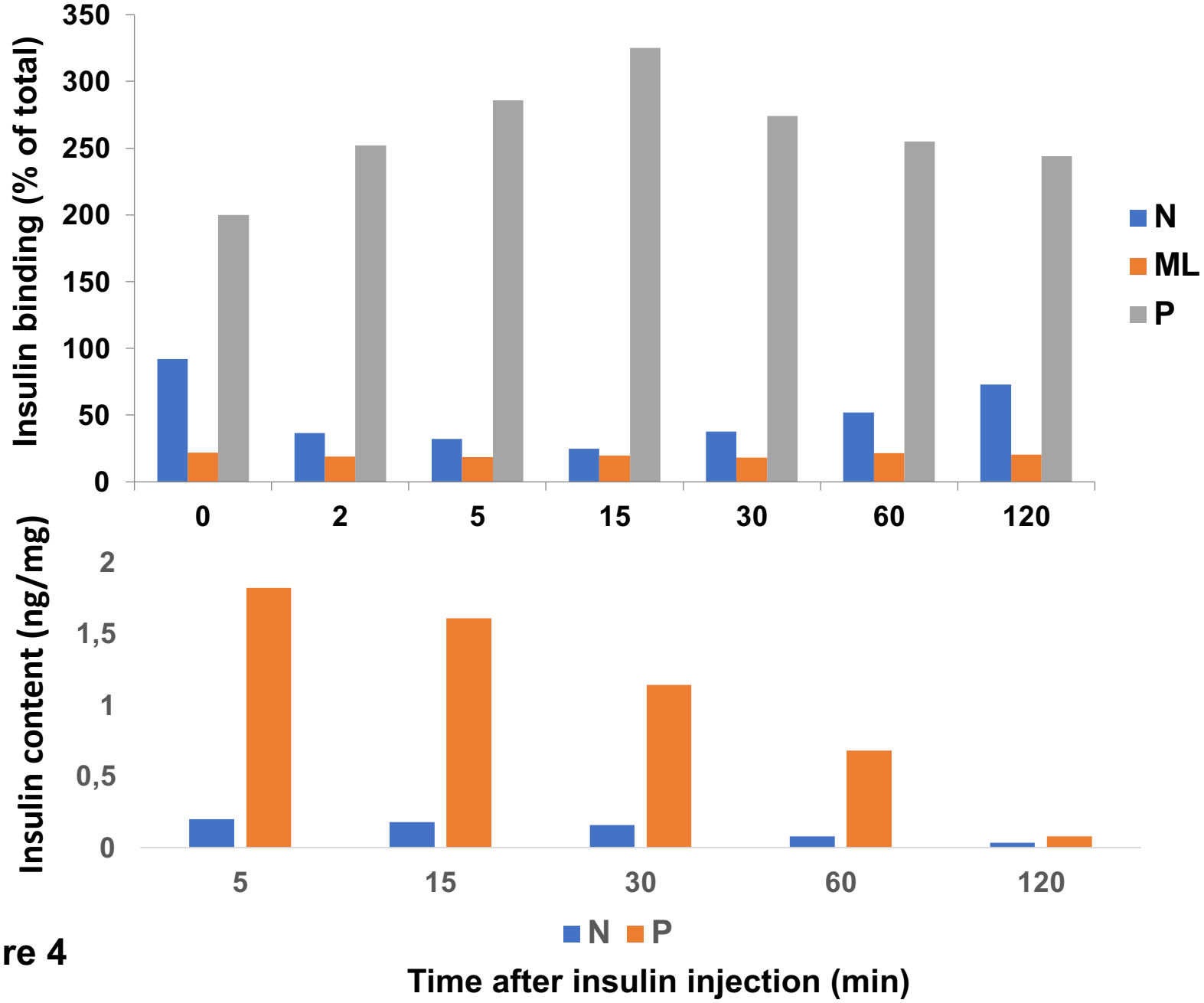
Insulin binding (% of total)
350
300
250
200
150
100
50
0
0
2
5
15
30
60
120
N
ML
P
Insulin content (ng/mg)
2
1,5
1
0,5
0
5
15
30
60
120
N
P
Time after insulin injection (min)

Figure 4

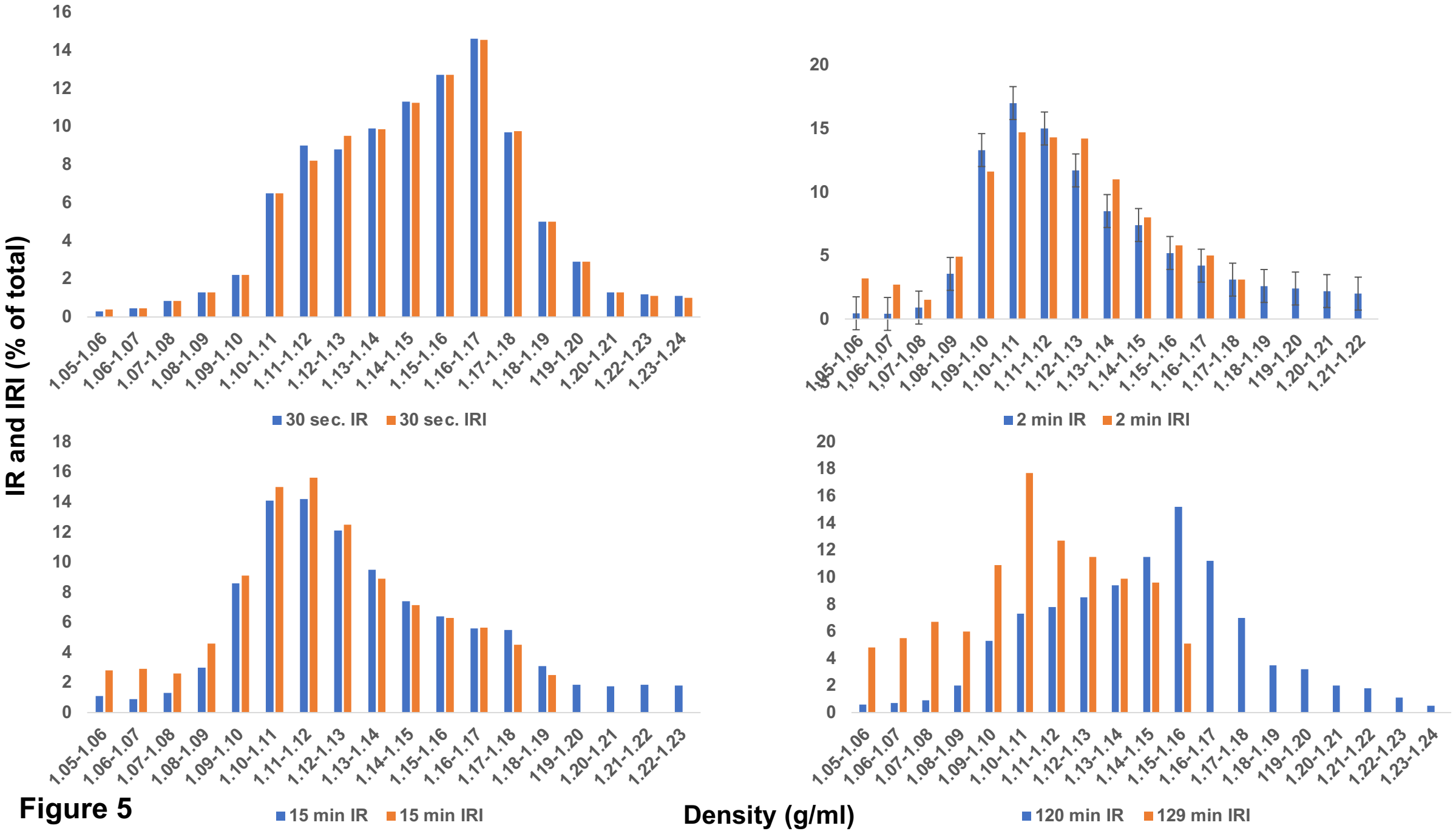
IR and IRI (% of total)
30 sec. IR
30 sec. IRI
2 min IR
2 min IRI
15 min IR
15 min IRI
120 min IR
129 min IRI
Density (g/ml)

Figure 5

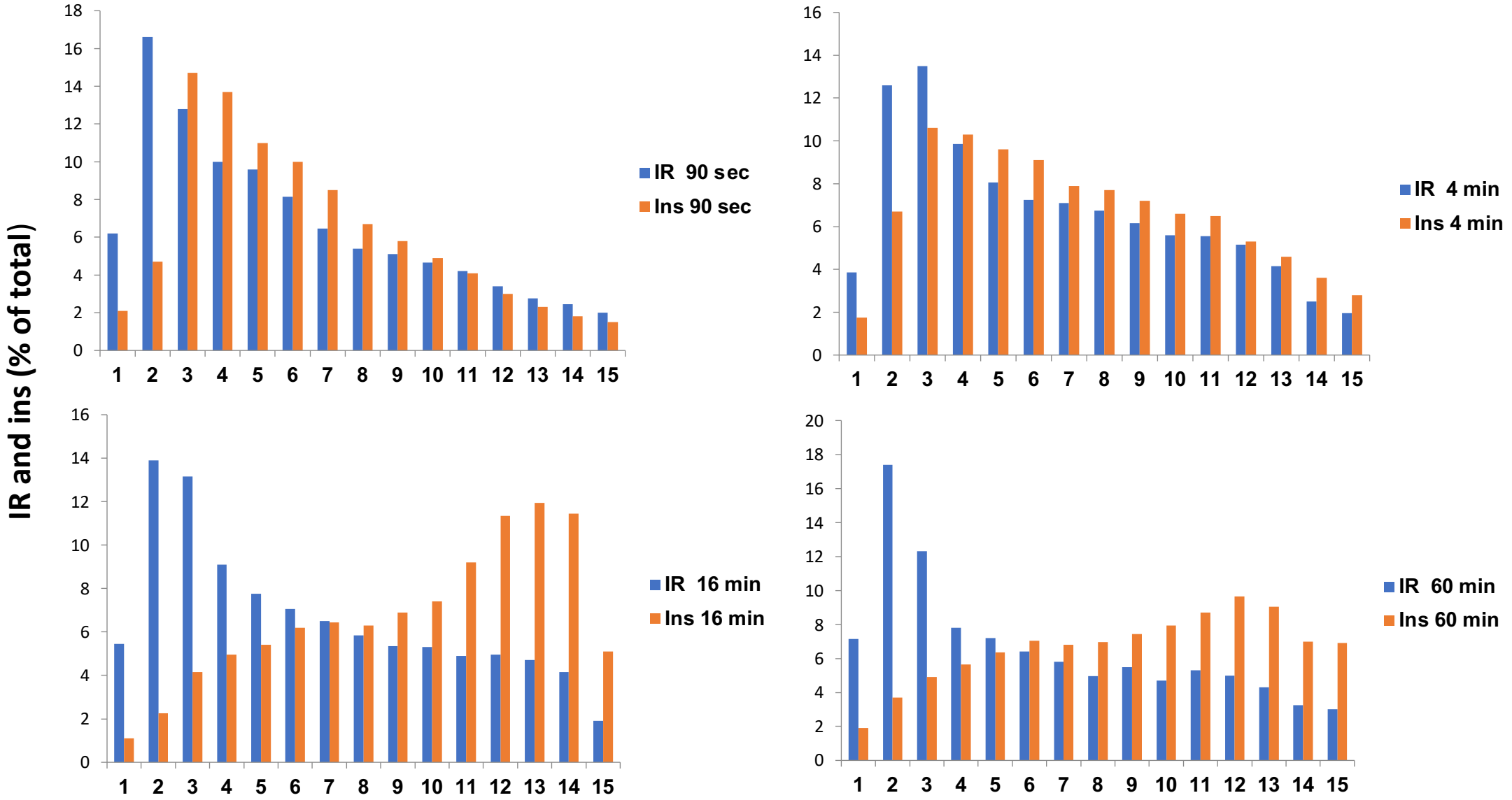

Figure 6

Fraction number

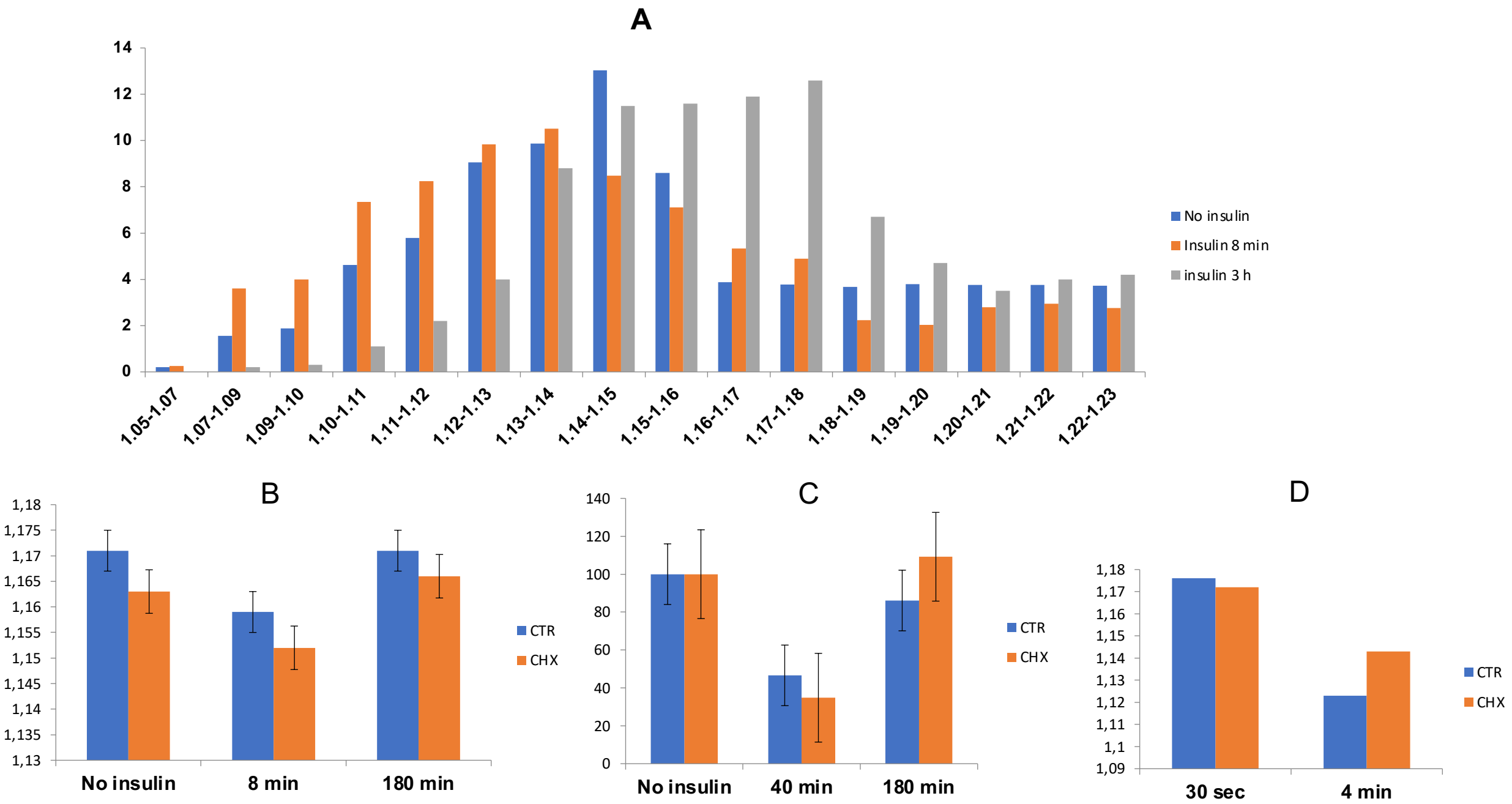
A
14
12
10
8
6
4
2
0
1.05-1.07
1.07-1.09
1.09-1.10
1.10-1.11
1.11-1.12
1.12-1.13
1.13-1.14
1.14-1.15
1.15-1.16
1.16-1.17
1.17-1.18
1.18-1.19
1.19-1.20
1.20-1.21
1.21-1.22
1.22-1.23
No insulin
Insulin 8 min
insulin 3 h
B
1,18
1,175
1,17
1,165
1,16
1,155
1,15
1,145
1,14
1,135
1,13
No insulin
8 min
180 min
CTR
CHX
C
140
120
100
80
60
40
20
0
No insulin
40 min
180 min
CTR
CHX
D
1,18
1,17
1,16
1,15
1,14
1,13
1,12
1,11
1,1
1,09
30 sec
4 min
CTR
CHX

Figure 7

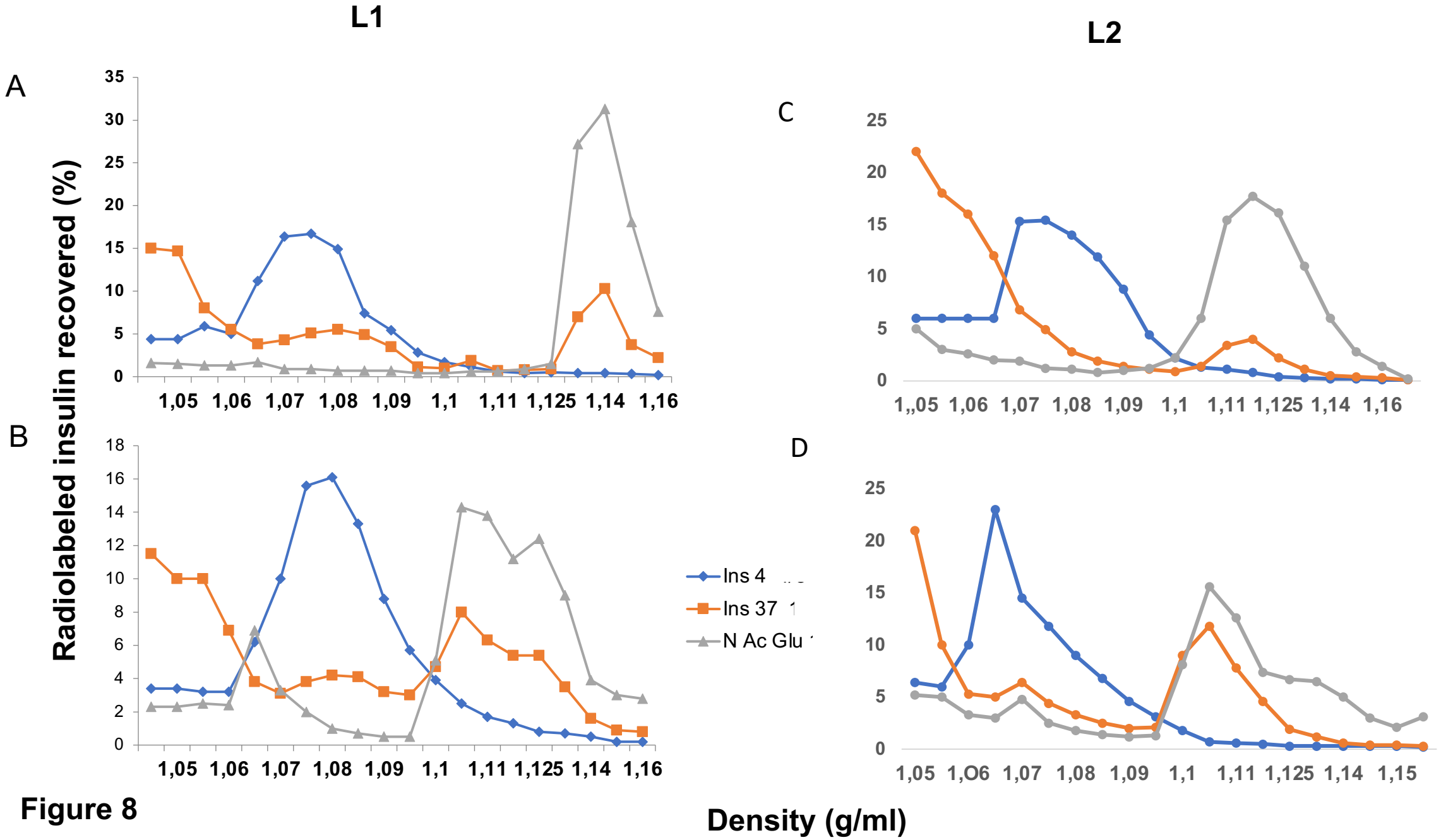
L1
L2
A
B
C
D
Radiolabeled insulin recovered (%)
Ins 4
Ins 37
N Ac Glu
Density (g/ml)
1,05 1,06 1,07 1,08 1,09 1,1 1,11 1,125 1,14 1,16
1,,05 1,06 1,07 1,08 1,09 1,1 1,11 1,125 1,14 1,16
1,05 1,O6 1,07 1,08 1,09 1,1 1,11 1,125 1,14 1,15

Figure 8

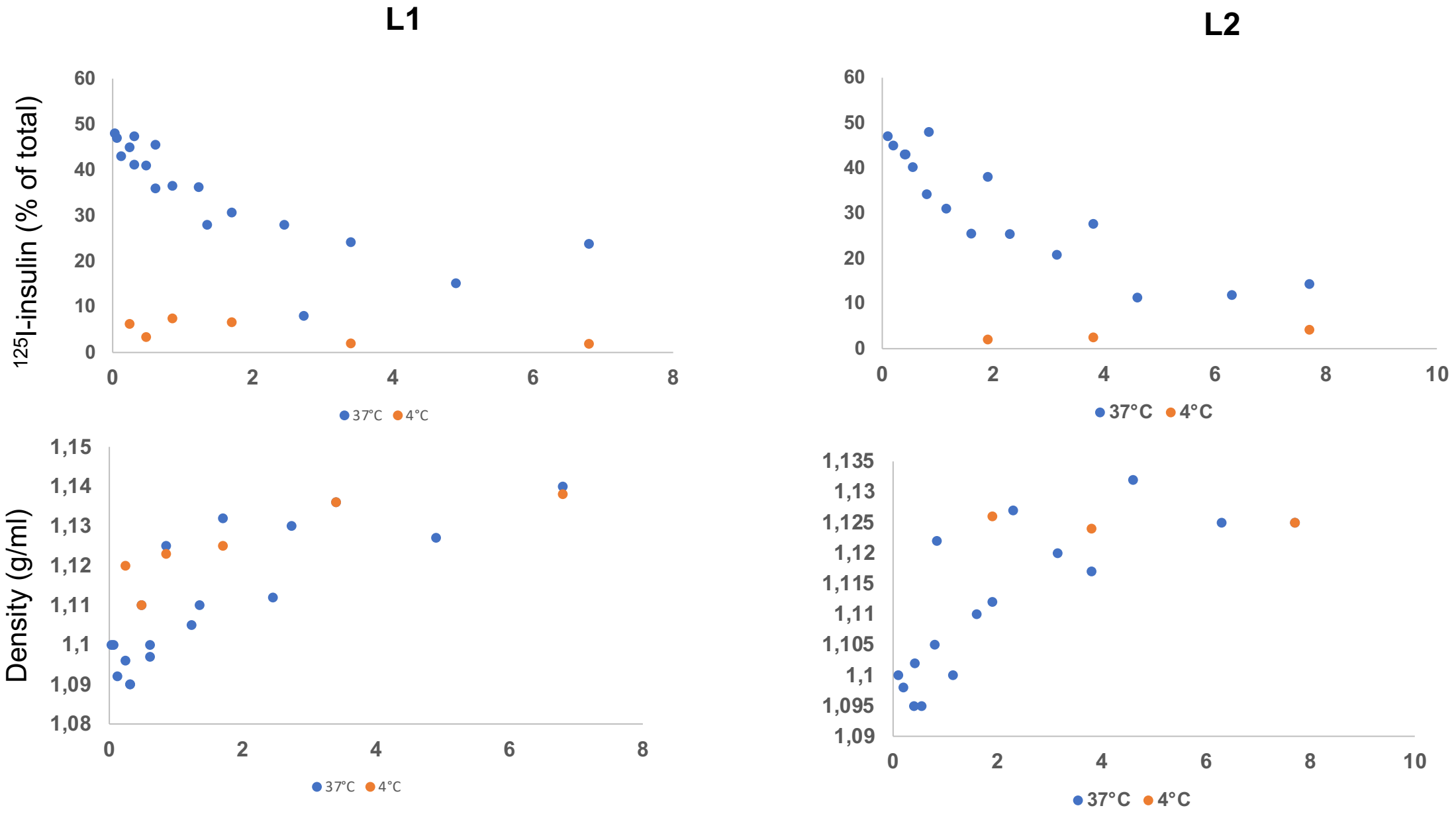
L1
L2
125I-insulin (% of total)
Density (g/ml)
37°C
4°C
Lysosomal / endosomal protein ratio

Figure 9

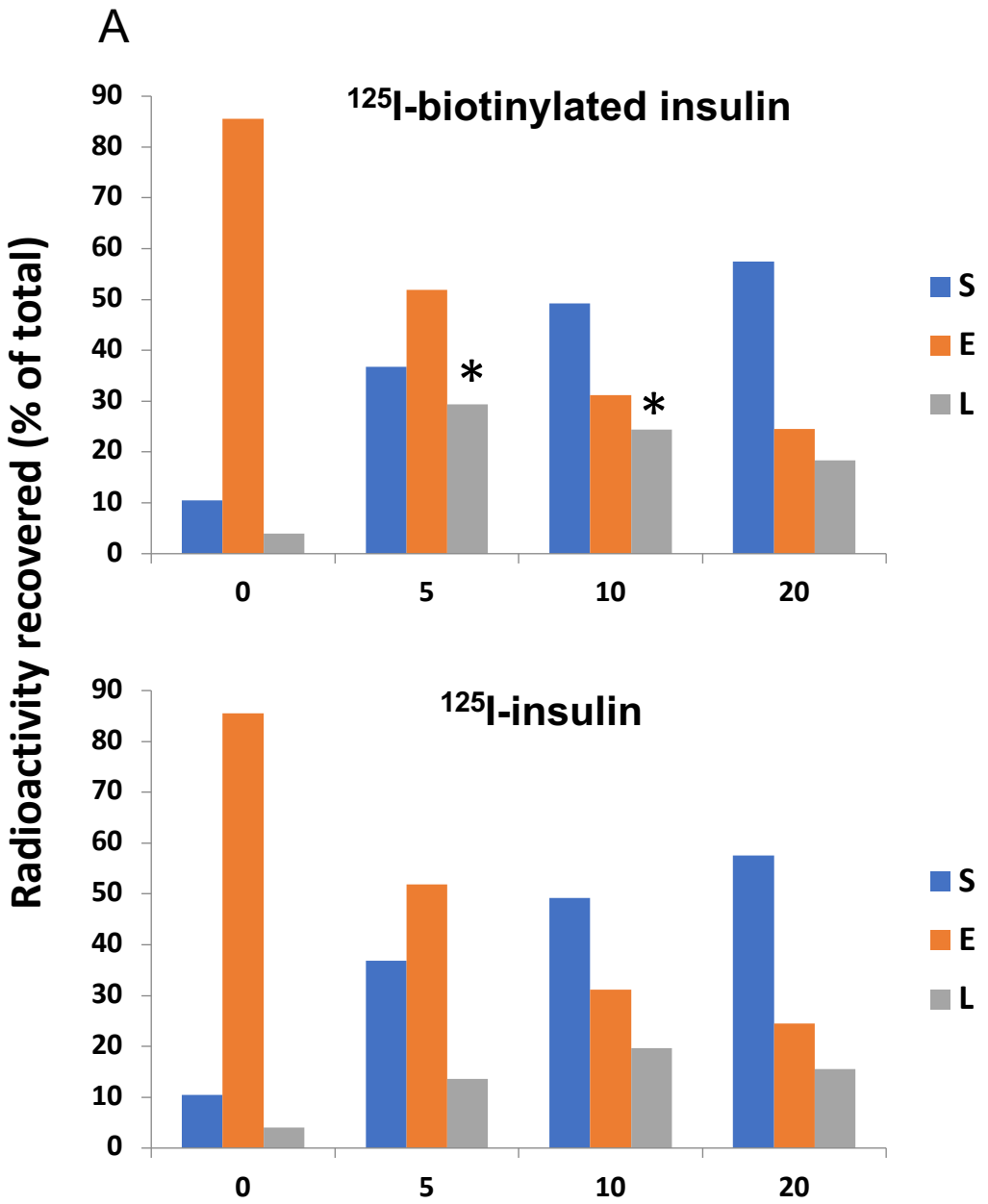
A
125I-biotinylated insulin
125I-insulin
Radioactivity recovered (% of total)
Time (min)
S
E
L
*
*
0
5
10
20
0
10
20
30
40
50
60
70
80
90

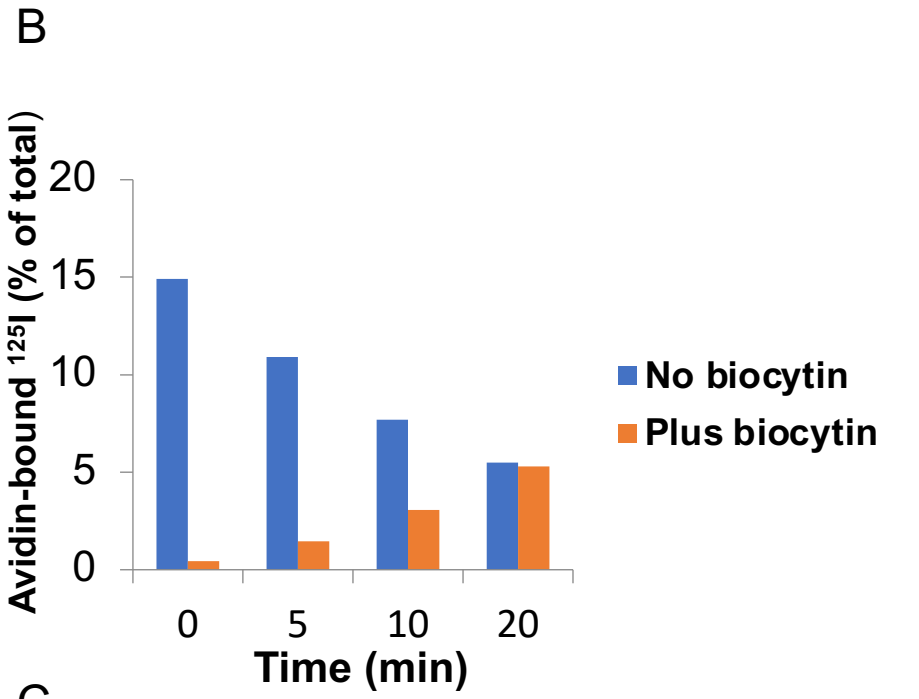
B
Avidin-bound 125I (% of total)
Time (min)
No biocytin
Plus biocytin
0
5
10
15
20

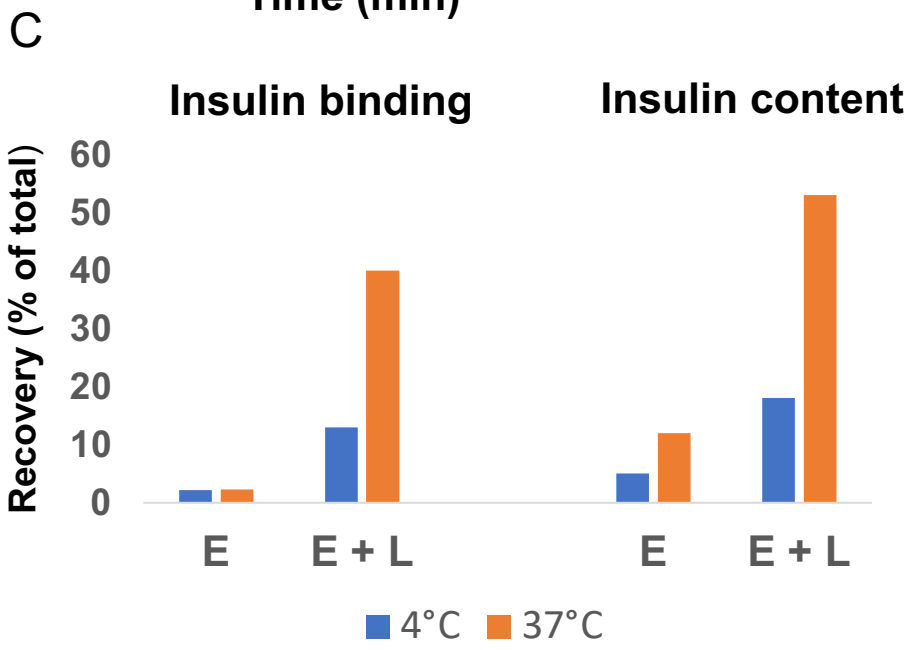
C
Insulin binding
Insulin content
Recovery (% of total)
E
E + L
E
E + L
4°C
37°C
0
10
20
30
40
50
60

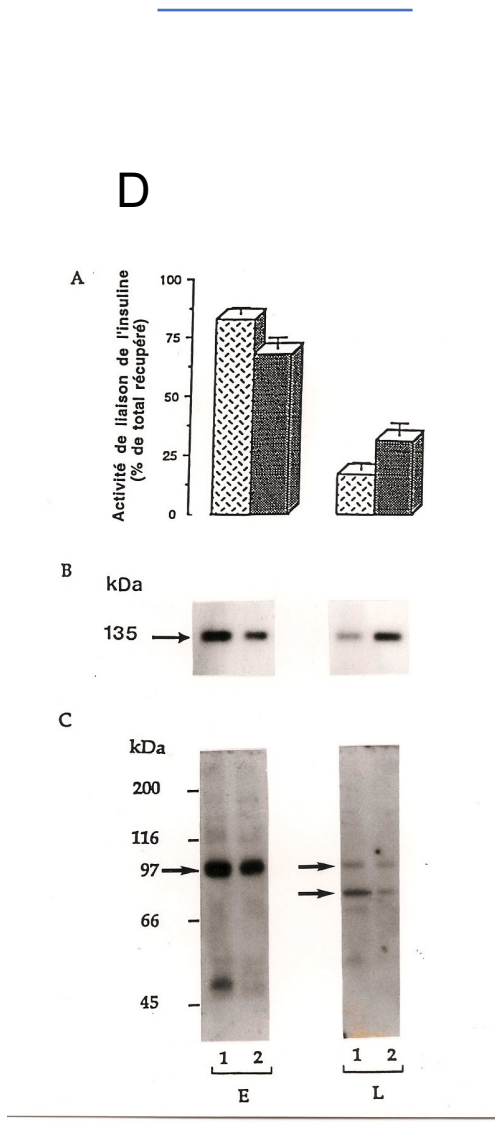
D
A
Activité de liaison de l'insuline (% de total récupéré)
100
75
50
25
0
B
kDa
135
C
kDa
200
116
97
66
45
1 2
E
1 2
L

Figure 10